NTNU

Norwegian University of
Science and Technology

Optimal Voltage Control of the Southern Norwegian Power Grid

Mixed Integer Nonlinear Programming (MINLP) for Control and Optimization of the High Voltage Southern Norwegian Power Grid

Erik Lundegaard Hannisdal

Master of Science in Engineering Cybernetics
Submission date: June 2011
Supervisor: Bjarne Anton Foss, ITK

Norwegian University of Science and Technology
Department of Engineering Cybernetics

Problem description

Statnett is, by virtue of having system responsibility of the Norwegian high voltage power grid, responsible for keeping the voltage at an acceptable level. Keeping the right voltage level is important to ensure good security of supply, long component lifetime and limit the transmission losses in the network.

In the modern deregulated power grid, the power flow changes more and faster than ever before, new large cables for import and export contributes to amplify this development by putting pressure on the transmission limits. These factors make a modernization of the voltage control scheme a requirement, which is today, to a great extent, manual.

A model and optimization based control system opens possibilities for improving the voltage control. This hypothesis is the starting point for this master thesis.

During the work of the master thesis the candidate will develop and analyze an optimization based control algorithm for voltage control in the Southern Norwegian high voltage power grid with the following qualities:

- Handle continuous and discrete control components.
- Minimize power system loss, while maintaining the voltage levels.
- Minimize the number of control actions.
- Perform simulations to show and verify the validity of the algorithm.
- Analyze and compare the algorithm to alternative control schemes.

The master thesis will be based on the candidates work on power system modeling performed in the specialization project during fall 2010.

Assignment given: January 10th 2011

Supervisor: Bjarne Anton Foss, ITK

Co-Supervisor: Eivind Lindeberg, Statnett SF

Abstract

This thesis contains the synthesis, analysis and simulation results of an automatic optimal voltage controller for the Southern Norwegian power grid. Currently the high voltage power grid is controlled manually by operators switching control components. The optimal controller handles the voltage control of the system, as well as keeping the number of control actions to a minimum.

The system model is derived from power system analysis. Due to a highy nonlinear system model and integer decission variables in on/off control components, the controller is based on mixed integer nonlinear programming (MINLP). The MINLP uses BONMIN as a solver, and is implemented with the AMPL programming language.

It was found that a MINLP controller is good choice for voltage control in transmission systems. The controller handles voltage limits, as well as reducing the number of control actions.

The thesis also contains comparison between different solution methods for applying the optimal voltage controller, as well as other approaches to the automatic voltage control problem.

Preface

This thesis was written in collaboration with Statnett SF and the Department of Engineering Cybernetics at the Norwegian University of Science and Technology, and is part of a paradigm shift towards fully automated voltage control in the Norwegian high voltage power system.

My initial introduction to the power transmission community has a summer internship at Statnett. Observing the current status for voltage control inspired my work on improving the current situation. As a control engineer, taking on the task of controlling powers of this magnitude was inspiring.

Power transmission is an absolutely vital field when developing a greener and more sustainable power system. Being a part of reducing emissions and using our energy to the fullest was the main motivation for this thesis, as well as improving the current situations in terms of safety and security of supply in the high voltage power system.

I would like to thank my supervisor Professor Bjarne A. Foss for his useful advice and inspiring conversations, Øyvind Rui and Eivind Lindeberg at Statnett SF for their help on improving my understanding of power systems and my family for inspiring me to pursue a masters degree. I would also like to thank my lunch mates - "Brødkollektivet" - Ola Hjukse, Håvard Knappskog and Trygve Utstumo for comics relief during long office hours. A thank you is also in order to Wilhelm Fossen Haarstad for sticking by me during five years in Trondheim. Last, but not least, my thanks are extended to my girlfriend, Sara Halmøy Bakke, who brightens my day, even after long sessions of work on my thesis.

Trondheim, June 6, 2011

Erik Lundegaard Hannisdal

Contents

1 Introduction **1**
1.1 Smart grid . . . 3
1.1.1 Automatic voltage control as a component in a smart grid . . . 3

2 Background theory **5**
2.1 The high voltage power system . . . 5
2.2 Voltage control . . . 7
2.2.1 Electrical power . . . 7
2.2.2 Current situation . . . 9
2.2.3 Control structure . . . 10
2.2.4 Control components . . . 12
2.3 Optimization theory . . . 17
2.3.1 Problem formulation . . . 17
2.3.2 Mathematical optimization . . . 18
2.3.3 Solution algorithms . . . 19

3 Power system modeling **23**
3.1 Power flow model . . . 23
3.1.1 The power flow study as a good choice for voltage control . . . 23
3.1.2 Network Equations . . . 24
3.1.3 Chosen quantities in the different buses . . . 26

4 Problem formulation **29**
4.1 High voltage optimization problem 29
4.2 Cost function 31
4.2.1 Voltage limits 32
4.2.2 Reactive component switching 32
4.2.3 Cost of competing components 34
4.2.4 Weighting 35
4.3 Network model 35
4.3.1 Admittance matrix 37
4.3.2 Power flow 38
4.3.3 Modifying the network model for a decentralized controller 39
4.4 Constraints 40
4.5 Decision variables 40
4.6 Controller dynamics 41
4.7 Expanding the optimization problem 42
4.7.1 Including the continuous control components 42
4.8 Controller tuning 44
4.9 Physical simplifications 45
4.9.1 Choice of power lines 45
4.9.2 Reactive power from other electric components . . . 46
4.10 Control theoretical considerations 47
4.11 Simplifications to the optimization problem 47

5 Synthesis **51**
5.1 Solution platform 51
5.1.1 BONMIN 52
5.1.2 AMPL - A modeling language for mathematical programming 53
5.2 Initial conditions 53
5.2.1 Controller tuning 53
5.2.2 Starting points 56
5.2.3 Other requirements 56
5.3 System specifications 57

5.4 Simulation 58
5.4.1 Heavy - and light load case study 58
5.4.2 Monte Carlo simulation 59
5.5 MINLP in a decentralized controller 60

6 Results - Test cases **63**
6.1 Test cases 64
6.2 Light load test case 64
6.2.1 System model without SVCs 64
6.2.2 System model with SVCs 69
6.3 Heavy load test case 73
6.3.1 System model without SVCs 73
6.3.2 System model with SVCs 78

7 Results - Monte Carlo simulations **83**
7.1 Monte Carlo simulations 83
7.2 Centralized voltage control 86
7.2.1 System model with SVCs 87
7.2.2 System model without SVCs 96
7.3 Decentralized voltage control 104

8 Analysis **113**
8.1 Centralized optimization model 113
8.1.1 Test cases 113
8.1.2 Monte Carlo 115
8.2 Decentralized optimization model 116

9 Discussion **119**
9.1 Centralized MINLP controller 119
9.2 Comparison to other control schemes 120
9.2.1 Automatic, non-optimal controller 120
9.2.2 Distributed controller 121
9.3 Applicational considerations 121

10 Conclusion **123**

11 Further work **125**
11.1 Testing a full scale network 125
11.2 Future expansions 125
11.2.1 Smoother voltage levels 126
11.2.2 Time increasing voltage costs 126
11.2.3 Controllers 126

A Numerical values and power system theory **127**
A.1 Power flow equations 127
A.2 Per unit calculations 127
A.3 Line lengths 128
A.4 Test case power demands 128

B Scripts **131**
B.1 AMPL 131

Chapter 1

Introduction

In the modern society, electrical power drives the world around us. The focus on keeping emission down and reducing the climate changes are at the pinnacle of the rapidly increasing environmental concern. Development of new, sustainable energy sources are at constant growth. The Norwegian petroleum industry is exploring the possibilities of electrification of Norwegian Continental Shelf, the possibilities for exploiting offshore wind energy is growing and energy consumption is higher than ever.

More decentralized power generation, large power demands and generation at remote areas, and higher consumption; these factors all leads to higher demands for utilization of the power transmission network, which again leads to fluctuations in the voltage levels throughout the power grid.

This causes two major problems; if the consumption is low, the voltage level will increase to a point where the components (such as lines and transformers) will not be dimensioned for loads of such magnitude. This over capacity strain will lead to wear and tear of the components, which increases downtime, maintenance and decreases lifetime. On the contrary, if the consumption is high, the voltage level will drop and the power grid will eventually experience great losses of power in the lines due to the increased current (see section 2.2.1). It will ultimately not be able to deliver the power required from the system point of view, due to violations of operating ranges

in other equipment such as transformers.

The energy consumption varies a lot during the course of 24 hours; thus voltage control is a continuous task. In spite of the strong economic, environmental and safety benefits for automating the voltage control, this task in not fully automated at today's standards (although a pilot project is operating in the southern Norwegian region as this paper is written). The standard in today's voltage control scheme is operators monitoring the voltage levels throughout the regional high voltage power grid, and manually handling most of the voltage control. The goal is therefore to ultimately not only implement an automatic controller, but also an optimal controller to ensure the greatest economic, environmental and safety benefits, as well as increasing the security of supply.

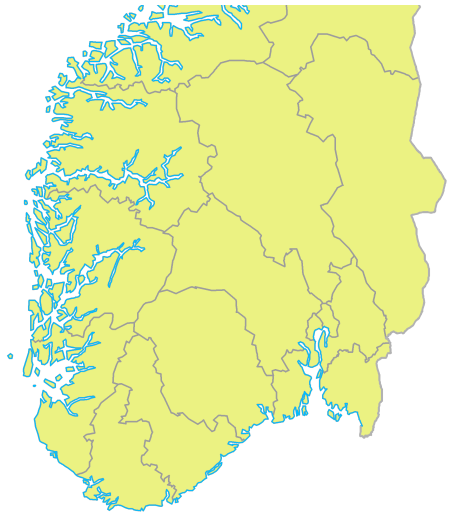

Figure 1.1: Map of South Norway, area of responsibility for the Southern Norwegian region

In this thesis the derivation of an optimal automatic voltage controller for the Southern Norwegian power grid is presented. The controller and

optimization algorithm uses the model presented in [14] as a basis. This model will also briefly be presented in this paper, see section 4.3. The model is a simplified representation of the current Southern Norwegian power grid.

1.1 Smart grid

Smart grid is the most popular term in current power transmission research and development, both nationally and worldwide. The Norwegian governments main focus has been automatic measurement - and control systems (AMS). This ensures that much of the customers consumptions will be moved to hours of the day with low loads [26]. Internationally, Pike Research reports that global investments on smart grid technologies will be about $ 200 billion between 2008 and 2015 [30].

Very briefly, the basic idea of smart grids is power systems using computer - and control technology to automatically control the energy efficiency or the power consumption and generation as a whole. This would mean that all elements in a power system is communicating, and thereby creating the opportunity for an optimal utilization of the power available in the network, both in terms of how it is produced and how it is distributed [8]. Smart grid uses both industrial components, such as smart instruments [27] and load control switches [6], and operational variables, such as prices, available producers etc. [8]

1.1.1 Automatic voltage control as a component in a smart grid

Even though most of the national media focus on smart grid is concentrated around energy consumers and producers, a lot of the potential for an efficient energy usage lies in the power transmission. Automating the voltage control in the power system is an important step for a coherent network. In line with the smart grid objective, automatic voltage control also provides more efficient energy usage, reduces the transmission losses and prepares the grid for more decentralized power generation. Current Norwegian energy politics (2011) supports the development of small-scale green power

plants. This is in accordance with green certificates allowing smaller environmentally friendly power plants to be economically sustainable in spite of high startup costs [31].

As other smart grid components, the main tool for implementing automatic voltage control is computer technology. Utilizing the possibilities of computer technology, automatic voltage control could over time be included in a centralized control scheme connecting the entire power system. By doing this, limits, weights and requirements for the voltage controller can be changed automatically according to the system wide optimal power demands.

Chapter 2

Background theory

2.1 The high voltage power system

Power transmission connects the power plants to the consumers. The majority of the power consumed in a geographical area (e.g. a nation, such as Norway) is generated centralized, such as in large dams, thermal - or nuclear power plants or wind mill parks [12]. In order to utilize this power, distribution is necessary. The main task of the high voltage power grid is therefore to distribute electrical power, while minimizing the amount of loss, as well as maintaining the security of supply [35].

Loss is the main reason for using a high voltage line, as opposed to distributing the power using lower voltages and higher currents. Ohm's law states that current and voltage is directly proportional between two points, and are inversely proportional to the resistance between them [15],

$$V = RI \tag{2.1.1}$$

It is also known that voltage and current are directly proportional to the power transferred [15], and inversely proportional to each other,

$$P = IV \tag{2.1.2}$$

Combining equations (2.1.1) and (2.1.2), yields $P = I^2R$. This means a reduction in current will give a squared reduction in resistive power loss in a transmission line.

The Norwegian high voltage power grid consists mainly of overhead lines. Nominal voltage levels are between $132kV$ and $420kV$, all new power lines and almost all power lines in southern Norway are $300kV$ or $420kV$. The transmission lines use three-phase alternating current (AC), which is the case in most transmission lines worldwide [22, 35].

The frequency of the Nordel power system[1] is set at $50Hz$. This is not a necessity, but a tradeoff between acceptable loss (higher frequency gives greater loss) and acceptable transforming abilities (lower frequency means larger and more expensive transformer stations).

In Norway, 96 % of all power generation is hydropower [25]. Hydropower has many advantages, it is relatively cheap (after a dam or other hydroelectric construction is built) and the power plant does not need additional resources other than for maintenance and supervision. It is also very friendly to the environment, as its energy is both free of CO_2 emissions and completely renewable.

Hydropower presents greater controllability than what is possible with thermal power plants. A thermal power plant has to run at full power continuously to be most effective [13]. This means that is produces the same amount of power during the day as is does during the night. Due to the controllability of hydropower plants, the Norwegian power demands are covered by import from continental Europe during the night, when energy is cheap. This means the potential energy in the impounding dams will remain, which again leads to an export of power during the day, to cover the excess demands in continental Europe, when prices are high. This import and export of power is mainly done through HVDC (High Voltage Direct Current) cables from the south of Norway across Skagerrak and the North Sea [40]. This will lead to a severe change in power demands, and voltage oscillations, over the course of 24 hours.

[1] The Nordel power system is a synchronous power grid that spans over Norway, Sweden, Finland and parts of Denmark [24]

From a control point of view, the controllability of the hydropower plants presents a challenge. The combination of numerous small power plants and the fact that they are unpredictable in terms of when - and how much energy is produced, leads to a control problem with more uncertainty and a lot of disturbance (fluctuations in the generated energy will be considered disturbances, given that these are uncontrollable variables for Statnett).

2.2 Voltage control

As mentioned in section 2.1, the voltage level experience severe fluctuations over the course of 24 hours. In order to maintain reasonable operating conditions, and reduce losses in the transmission, control of the voltage level is needed.

2.2.1 Electrical power

The majority of this section on electrical power can be found in [14]. The controlling factor for voltage control is not the real power, but the reactive power. If the generation of reactive power is too low relative to the absorption, the voltage level drops and vice versa [22].

φ is the phase difference between the current and the voltage, as shown in figure 2.1. To improve the power factor (denoted as $cos\ \varphi$), the sum of the absorption and generation of reactive power should be as close to zero as possible, i.e. $cos\ \varphi \approx 1$. This will lead to a greater utilization of the power, where the real power is close to the apparent power, and that current and voltage has a small difference of phase.

Figures 2.2 shows the relationship between apparent -(S), real -(P) and reactive power (Q), where

$$S = P + jQ \quad [MVA] \tag{2.2.1}$$

and

$$P = S\ cos\ \varphi \quad [W]$$
$$Q = S\ sin\ \varphi \quad [MVAr] \tag{2.2.2}$$

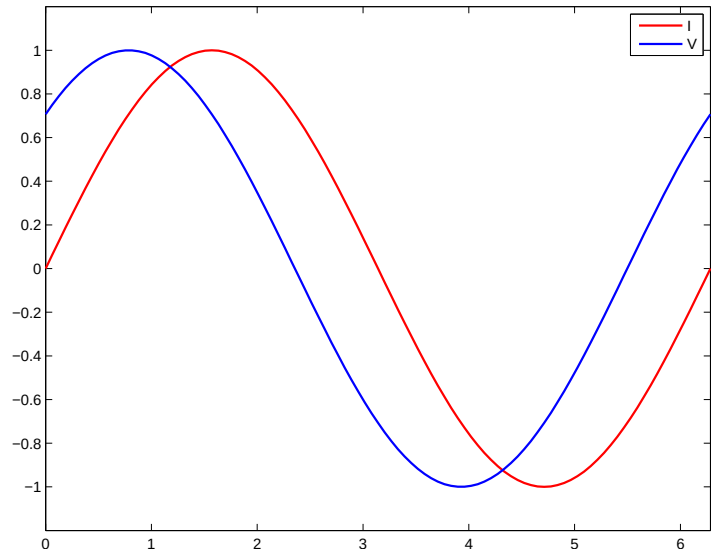

Figure 2.1: Voltage $[V]$ and current $[I]$, the voltage leads the current by a phase φ

Voltage control is done by adding and subtracting reactive power from the transmission network, to compensate for the reactive loss in a power line (see section 4.3.1), and thereby changing power factor. The network is equipped with components for producing and consuming reactive power to perform control, these are presented in section 2.2.4.

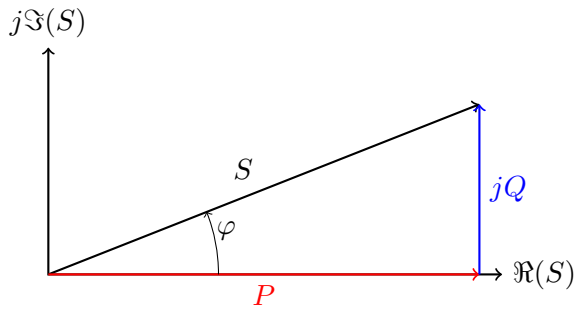

Figure 2.2: Complex Power

2.2.2 Current situation

Until recently, close to all voltage control in the Norwegian power grid was performed manually. The couplings done in a day is between 100 and 150 in the southern Norwegian region alone[2]. This number is increasing with the expansion of the grid, and so is the operator's additional work, as for example securing lines for maintenance. The added workload on the operators may lead to less focus on both voltage control and other assignments in the future. This could lead to even greater variations in the voltage, and possibly neglecting other important tasks, which in a worst case scenario, could lead to personal injury.

Due to these factors, Statnett chose to pursue an automated approach to handle the voltage control problem. Since spring 2011, the previously mentioned pilot project algorithm has been running on the regional central, coupling reactive components in and out according to the voltage limits. The current automatic voltage controller (ASK) is briefly explained in [14], and is based on logic functions deciding on reactive components couplings according to strict boundaries, i.e. the voltage limits.

Even though an automation algorithm already exists, the use of op-

[2]The facts and figures in this section is based on conversations with Statnett employees, summer/fall 2010.

timization and control theory in the algorithm can possibly improve the performance of the controller and help minimize controller actions that cause wear and tear on the components.

Optimization challenges

By implementing an optimal controller, the possibility to handle additional challenges regarding the voltage control presents itself.

As mentioned, most of the voltage control is done by switching reactive on/off components (for more, see section 2.2.4). These components will suffer great wear and tear with frequent switching, which means that the ideal switching scheme will keep the voltage levels, while still keeping the switching at a minimum.

The other important voltage controllers in the transmission network are the FACTS. In the Norwegian power grid, close to all FACTS are SVCs (for more on FACTS and SVCs, see section 2.2.4). SVCs are automatic voltage controllers and do not require manual actions other than setting the voltage setpoint. Even so, including the SVCs to the voltage control algorithm could give very desirable results. The SVCs are the components that handle sudden voltage changes, e.g. the fallout of a power line etc. By limiting the generation or consumption of reactive power in a SVC, i.e. keeping the SVCs further away from its operational limits, the safety will increase. The SVCs will then keep its ability to handle sudden changes in the voltage level, due to its reactive power potential.

2.2.3 Control structure

The majority of this section can be found in [14]. Voltage control is not an unexplored field, and is implemented in other countries. Even though there are many differences between what will be known as "The Norwegian Model" and the ones implemented today, there are also many similarities and general control structural methods that can be taken advantage of.

Generally the control structure is divided into three levels in a very hierarchical matter (sometimes four, but the principle is the same). The

different levels include:

Tertiary Voltage Control

(TVC) is the highest level in it structure. The objective is to find the ideal voltage level throughout the system, based on changes in operating conditions for the generators, demand, transmission etc.

This is done by the operators manually, but could be optimized using an optimization algorithm. If this was done, the time constant for an automated TVC would be about 10-20 minutes.

Secondary Voltage Control

(SVC[3]) is the next level in the hierarchy. The objective is to control the voltage in certain regions of the network. This level takes the setpoint from the TVC. The SVCs task is to distribute the generation and consumption of reactive power based on where it is needed.

In Norway the operator handle this as well at the current date, whoever this is getting to be very time consuming and is at the core of this control problem. A challenge with this control level is to divide these regions (or "zones" as the French call them) into more or less decoupled areas.

The time constant for this task would be about two minutes. This would be sufficient time for the voltage levels to stabilize based on the changes made by the controllers. This level is also meant to cope with the strong coupling problem in this control system. The challenge lies in finding the least coupled, or strongest decoupled, zones, as well as the actual optimization.

Primary Voltage Control

(PVC) is the control system for the reactive components. This is automated today (in closed loop) for some of the continuous/dynamic control compo-

[3]This is an unfortunate abbreviation given that Static Var Compensators (see section 2.2.4) uses the same. It is however used in existing literature and keeping the same standard desired.

nents (the FACTS devices). The automatic control of the generators will be the producers' responsibility; however the setpoint should come from the secondary voltage control, given the hierarchic buildup of the control system [36]. For more on generator voltage control, see [14, 34].

The on/off components are not considered a part of PVC, but a tool for the SVC. The on/off components does not operate in closed loop and will not follow a setpoint, they are, however, used as an input for the voltage control on a regional level as an input.

The PVC can be considered almost instantaneous with a time constant of only few seconds.

One can clearly see that even without the automated environment for voltage control, the hierarchical structure is still there. Voltage control is as much a coordination task as it is a general control problem. It is also clear that there needs to be a temporal and spatial independence between the level/layers [36]. [17, 29, 32, 33, 38]

In this paper it is chosen to look at a control scheme that connects both the top layers, i.e. the tertiary level and the secondary level, as well as a distributed model. Connecting the two top layers will be done by a fully centralized controller.

2.2.4 Control components

Voltage control in a power grid is performed by several manipulated variables. This section will summarize the most important ones. This is an extraction from a more detailed presentation given in [14].

Capasitor Banks

[22] A capacitor battery (several batteries in a bank), or a capacitor, is a purely capacitive component. It is used for production of reactive power. Capacitors are used when the voltage is too low. The component can only be used on or off; the reactive power produced by a capacitor battery

is fixed. A capacitor can be modeled as two metal plates with a non-conductive area between them. If there is a potential difference between them, an electric field is created, thereby storing energy.

Reactors

[22] A reactor, or an inductor, is a purely inductive component. It is used for consumption of reactive power. A reactor is therefore used when the voltage is too high. Some of the components can only be used on or off, in other words, the reactive power consumed by these reactors is fixed. Some can be controlled in a stepwise manner, the same way voltage control is executed by a transformer in a distribution system (by changing the tapping point [3]).

A reactor will have a time constant from a matter of seconds to a minute. An inductor can be modeled as windings of conducting wire. When current is sent through this material, energy is used to create a magnetic field around this coil.

FACTS

A Flexible Alternating Current Transmission Systems (FACTS) [28] device is used for power generation and consumption in a transmission system. For the voltage control application it is the shunt (parallel) connected devices that are of importance. These are the ones that generate and consume reactive power. A FACTS device usually operates at a lower voltage level than the high voltage power line, and is therefore fitted with a transformer for operational proposes. FACTS are dynamic devices, as opposed to on/off devices such as reactors and capacitor batteries.

A SVC (Static Var Compensator) [28] device is a shut connected FACTS device, and its purpose is to adjust the voltage of a given bus/node by adding inductive or capacitive current. A SVC consists of a TSC and a TCR in parallel.

Most of the FACTS devices found in the Norwegian power system are SVCs.

A TSC (Thyrsistor Switched Capacitor) generates reactive power, but the amount of MVAr generated is set, this is because there can be no steps in the voltage level over a capacitor as this would lead to a very high current ($i = C\frac{dV}{dt}$). Therefore the Thyrsistor valve ensures that this "side" of the SVC is either on or off.

A TCR (Thyrsistor Controlled Reactor) consumes reactive power and has the ability to control the amount consumed by the reactor. This is done in a continuous matter by a partial conduction of a thyrsistor valve (triac). The triac is connected to a power supply controlled by a controller that takes the measured voltage level, V, as an input.

By utilizing both the TSC and the TCR, the SVC is able to generate or consume as much reactive power as needed (within its bounds).

There are also components in the network that only utilize the TCR part of the SVC. This is typically for lines that are strongly capacitive, such as underwater cables (for example the Rød - Hasle connection [14].

Figure 2.4, shows the V-Q characteristics for the SVC. It can be seen that for voltages below the reference voltage the Q-value is positive, and by that the SVC is capacitive. For voltages above the reference the Q-value is negative and the SVC inductive. A block diagram of the SVC-model is shown in figure 2.3.

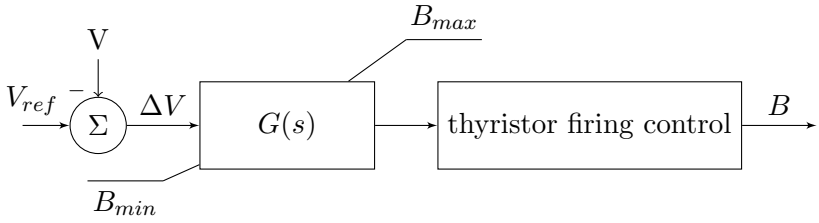

Figure 2.3: [14] Block diagram for a SVC

The transfer function $G(s)$ when $s \to 0$ i.e. $t \to \infty$ is given by

$$G(s)|_{s=0} = K \tag{2.2.3}$$

Which again means that, in steady-state, the change in susceptance (explained in section 3.1) is proportional to the change in voltage, $\Delta B = K\Delta V$. It is also known that the change in reactive power is given by: $\Delta Q = \Delta B V^2$. So for voltages around the reference (indicated by I in figure 2.4),

$$\Delta Q \cong (KV_{ref}^2)\ \Delta V. \tag{2.2.4}$$

In the part noted by II and III it is the max and min values, respectively, of susceptance that limit the Q value, which mean that Q is proportional to the square of the voltage level, $Q = B_{MAX}V^2$ for II, and $Q = B_{MIN}V^2$ for III.

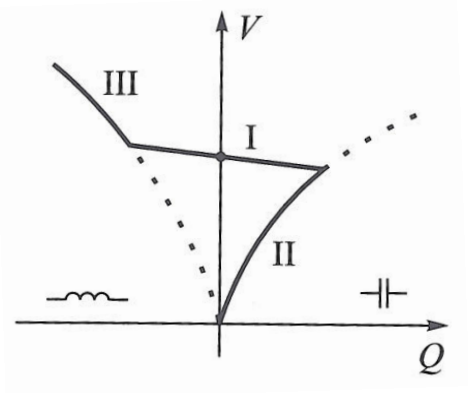

Figure 2.4: $V - Q$-diagram for a SVC [19]

STATCOM (Static Synchronous Compensator) [28] is an alternative to the SVC device. It is also a shunt connected FACTS device, which only controls the reactive -, not the real power.

The STATCOM has a VSC (voltage source converter) coupled in parallel with a power supply with a controller that takes the measured voltage level $V_{STATCOM,Measured}$ as an input.

The VSC is basically a DC to three phase AC converter that determines the desired phase, amplitude and frequency of the signal. Using this application the STATCOM is able to both generate and absorb reactive power by alternating the phase of the voltage.

Figures 2.5 and 2.6 shows the V-I and V-Q characteristics for the STATCOM respectively. As seen, the current will remain constant at a voltage with considerable deviations from the reference. This will lead to the linear characteristics seen both above and below the voltage reference in figure 2.6 ($Q = VI_{min}$ and $Q = VI_{max}$).

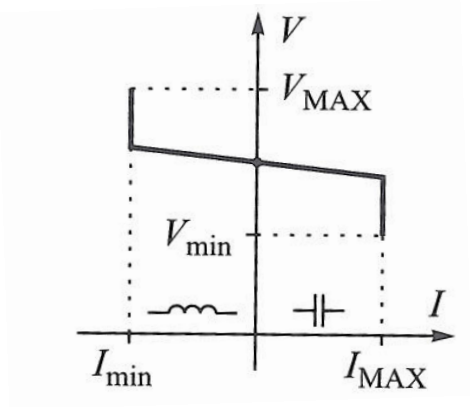

Figure 2.5: $V - I$-diagram for a STATCOM [19]

The basis for automating the voltage control is to use the power flow equations as a model for the physical characteristics in the power grid.

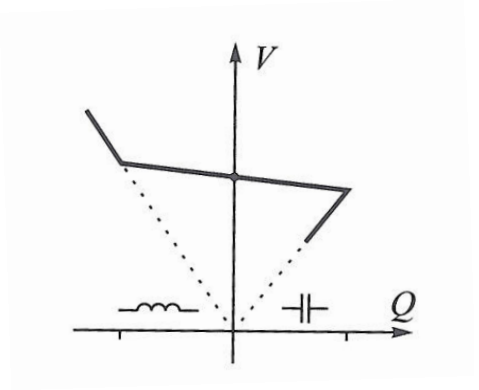

Figure 2.6: $V - Q$-diagram for a STATCOM [19]

2.3 Optimization theory

To find the optimal scheme for the voltage control components, optimization theory is applied. Basic optimization theory is assumed known to the reader and can be found in detail in [23, 43]. Still, a quick run-through of the most important points used in this thesis will be presented.

2.3.1 Problem formulation

An optimization problem consists of the following three main points:

1. An objective function that formulates a maximization or minimization objective.

2. Constraints that limits the problem to exceed bounds set by physical laws, economic boundaries or other limits.

3. Decision variables that should be manipulated to achieve the optimal solution.

The mathematical formulation will be as follows [23]:

$$\begin{aligned} \underset{x \in \mathbb{R}^n}{\text{minimize}} \quad & f_0(x) \\ \text{subject to} \quad & c_i(x) \geq 0, \ i \in \mathcal{I} \\ & c_i(x) = 0, \ i \in \mathcal{E} \end{aligned} \tag{2.3.1}$$

Where $\mathcal{I}$ and $\mathcal{E}$ and set of indices for inequality and equality constraints, respectively.

2.3.2 Mathematical optimization

There are several types of optimization problems, which are expressed and solved in different manners. Only the ones used in the thesis will be presented briefly.

Nonlinear programming

Nonlinear programming as characterized by a nonlinear problem formulation, either a nonlinear objective function or constraints. Nonlinearities may lead to non-convex problems. Non-convex problems presents a challenge in that when an optima is found, a guarantee cannot be made to whether this is the global - or only a local optimum.

Integer programming

As opposed to optimization problems using continuous variables, integer programming presents some challenges. Solving optimization problems using continuous variables relies generally on finding the derivative of the function, and uses this to move towards the optimum. However, using integer programming, no derivative can be provided, therefore the solution algorithms used have to be built up in an entirely different way.

Mixed Integer NonLinear Programming (MINLP)

Mixed integer nonlinear programming combines the challenges of the previous tasks by including both nonlinearities and integer decision variables. And is by that the hardest, and most time consuming optimization problem to solve. Given the complexity of MINLP the details will not be given in this thesis, as its focus is mainly solving the Southern Norwegian high voltage control problem. For the curious reader, details can be found in [7]. A general formulation of MINLP:

$$\begin{aligned} \underset{x\in\mathbb{Z}^n, y\in\mathbb{R}^n}{\text{minimize}} \quad & f_0(x,y) \\ \text{subject to} \quad & c_i(x,y) \geq 0,\ i \in \mathcal{I} \\ & c_i(x,y) = 0,\ i \in \mathcal{E} \end{aligned} \tag{2.3.2}$$

Where $\mathcal{I}$ and $\mathcal{E}$ and set of indices for inequality and equality constraints, respectivly and $\mathbb{Z}^n$ are all *integer* points on $\mathbb{R}^n$.

2.3.3 Solution algorithms

Solving an optimization programs require a set of rules. Solution algorithms are generally built up as iterative methods, starting at either a random - or given point and converging toward what is hopefully the optimum for the given program. The rules for taking these steps vary according to the nature of the optimization program. A continuous problem formulation will for example usually use an algorithm where the steps are taken based on the first - or second derivative of either the objective function or the constraints. An integer program will on the other hand require different approaches, as a discrete function does not have a derivative [23].

This section will very shortly go through the algorithms used for the voltage control problem.

Interior point

Solving nonlinear programs can be solved in different ways; the algorithm that solves the high voltage control problem uses the interior point method. The interior point method handles continuous problems. It searches for a better solution based on the gradient. As opposed to many other algorithms, the interior point method iterates toward the optimal point from either inside - or outside the feasible region, not on the boundaries. The interior point method generally used few "expensive" iterations rather than many "inexpensive". [23]

Branch and Bound

The branch and bound algorithm is one of the most common solution algorithms for non-continuous problems (integer programming, mixed integer programming or binary programming). The branch and bound method maps out possible solutions by placing them in a search tree. Upper and lower bound of possible solutions is found, and if the bounds indicates that any solution found by continuing down that given subtree is either infeasible or will not be the optimal solution, the rest is discarded.

The bounds are determined by using other solution algorithms on a relaxed optimization problem. For example, an integer problem is relaxed by setting one of the integer decision variables to an integer value and making the rest continuous. The best possible solution of the relaxed problem is therefore at least as good as the best integer solution in the same relaxed problem. Repeating this, the best possible solution and best found integer solution will ultimately converge to the same value.

Figure 2.7 shows an example picture of a nonlinear search tree, as seen the number of braches can become immense.

Branch and Cut

Brach and cut uses the same search tree structure as the branch and bound method and most of the algorithm consists of the same steps as branch and bound. The algorithm is used for solving MILPs (mixed integer linear

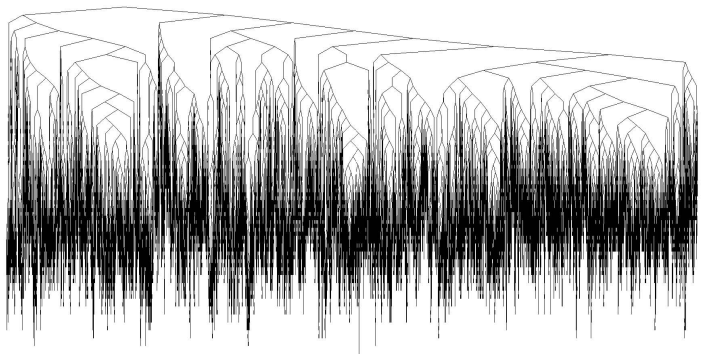

Figure 2.7: Example of a MINLP search tree [18]

programs). Branch and cut can be considered a special case of the branch and bound algorithm, where the LP relaxations are solved using the simplex method (for more on the simplex method, see [23]).

After an non-integer optimal solution is found a cutting plane algorithm is used to impose constraints that keep all integer points feasible, however not the current, non-integer, solution. [10]

Pseudo code and more details on the solution algorithms used by BONMIN (see section 5.1.1) is found in [2].

Chapter 3

Power system modeling

3.1 Power flow model

This chapter is to a great extent obtained from the specialization project, for more details see [14]. The timescale of system wide optimal control for a system of this magnitude will be high. The dynamic effects in a power system and in a transmission line [19] will therefore play a small role when modeling the power system. The main goal is to model the actual operating points, in steady-state.

There are many ways to mathematically represent a power network. Due to the timescale in question, and the fact that it is preferable to look at the power considerations as well as the voltage changes, a power flow study (or load flow study) is elected to be used as the model for the power grid.

3.1.1 The power flow study as a good choice for voltage control

The power flow study is used as a simplification of the power grid. In a power system it is neither economically sound nor practical to model the whole physical network. Therefore a power flow study is used. Generally the power flow model is used for planning a power grid, and for stead-

state analysis of the power grid [15]. Due to the power flow characteristics, the connections between the different buses become apparent and the voltage level will respond to changes in other buses (or nodes - meeting place for electrical components [21]). The characteristics include; modeling the power system as a whole and looking at the different buses in connection to each other.

3.1.2 Network Equations

All buses in an electrical network are linked. Therefore it is possible to derive a model for the coupling between the buses using a π-equivalent model (see section 4.3.1). Combining each individual model gives the nodal network equation:

$$\begin{bmatrix} \underline{I_1} \\ \vdots \\ \underline{I_i} \\ \vdots \\ I_n \end{bmatrix} = \begin{bmatrix} \underline{Y_{11}} & \cdots & \underline{Y_{1i}} & \cdots & \underline{Y_{1N}} \\ \vdots & \ddots & \vdots & & \vdots \\ \underline{Y_{i1}} & \cdots & \underline{Y_{ii}} & \cdots & \underline{Y_{iN}} \\ \vdots & & \vdots & & \vdots \\ \underline{Y_{N1}} & \cdots & \underline{Y_{Ni}} & \cdots & \underline{Y_{NN}} \end{bmatrix} \begin{bmatrix} \underline{V_1} \\ \vdots \\ \underline{V_i} \\ \vdots \\ V_n \end{bmatrix} \quad or \quad \underline{\mathbf{I}} = \underline{\mathbf{YV}} \tag{3.1.1}$$

Where $\underline{V_i}$ is the voltage at bus i, $\underline{I_i}$ is the current injection at bus i (which is the sum of all currents terminating in bus i) and $\underline{Y_{ij}}$ is the mutual admittance between buses i and j. More information is found in [19].

Fortunately most elements in $\underline{\mathbf{Y}}$ are zero, given that there must be a branch linking bus i and j for the element to be non-zero.

Using polar coordinate notation (for the generally written: $\underline{V_i} = V_i \angle \delta_i$ and $\underline{Y_i} = Y_{ij} \angle \theta_{ij}$) and the current injection for any bus:

$$\underline{I_i} = \underline{Y_{ii}}\underline{V_i} \; + \sum_{j=1; j \neq i}^{N} \underline{Y_{ij}}\underline{V_j}, \tag{3.1.2}$$

Then the following is obtained:

$$\begin{aligned}\underline{S}_i &= P_i + jQ_i = \underline{V}_i \underline{I}_i^* \\ &= V_i e^{j\delta_i} \left[Y_{ii} V_i e^{-j(\delta_i+\theta_{ii})} + \sum_{j=1;j\neq i}^{N} V_j Y_{ij} e^{-(\delta_j+\theta_{ij})} \right] \\ &= V_i^2 Y_{ii} e^{-j\theta_{ii}} + V_i \sum_{j=1;j\neq i}^{N} V_j Y_{ij} e^{j(\delta_i-\delta_j-\theta_{ij})}\end{aligned} \tag{3.1.3}$$

Which gives the following for the real and reactive power:

$$\begin{aligned}P_i &= V_i^2 Y_{ii} cos\ \theta_{ii} + \sum_{j=1;j\neq i}^{N} V_i V_j Y_{ij} cos(\delta_i - \delta_j - \theta_{ij}) \\ Q_i &= -V_i^2 Y_{ii} sin\ \theta_{ii} + \sum_{j=1;j\neq i}^{N} V_i V_j Y_{ij} sin(\delta_i - \delta_j - \theta_{ij})\end{aligned} \tag{3.1.4}$$

Alternatively the real and reactive power can be given by (derivation can be found in [19]):

$$\begin{aligned}P_i &= V_i^2 G_{ii} + \sum_{j=1;j\neq i}^{N} V_i V_j \left[B_{ij} sin\ (\delta_i - \delta_j) + G_{ij} cos\ (\delta_i - \delta_j) \right] \\ Q_i &= -V_i^2 B_{ii} + \sum_{j=1;j\neq i}^{N} V_i V_j \left[G_{ij} sin\ (\delta_i - \delta_j) - B_{ij} cos\ (\delta_i - \delta_j) \right]\end{aligned} \tag{3.1.5}$$

Where G_{ij} (conductance) and B_{ij} (suseptance) are the real and imaginary part of $\underline{Y}_{ij}$, respectively ($\underline{Y}_{ij} = G_{ij}+\mathrm{j}B_{ij}$). This is the notation used in the optimal voltage control problem.

Due to ohmic impedance (resistance) in the power lines, the total generation of real power will be larger than the total consumed in the different buses. This can be considered losses in the power lines.

$$\sum_{i=1}^{N} P_i = P_{loss} > 0 \tag{3.1.6}$$

Being modeled as π -equivalents (see section 4.3.1), there will also be inductive effects around the power lines. This means that the total generation of reactive power in the buses, due to reactive shunt components and generated reactive power by generators, will be larger than the reactive power consumed in the buses.

$$\sum_{i=1}^{N} Q_i = Q_{line\ inductance} > 0 \tag{3.1.7}$$

More details on the admittance in the power lines will be presented in section 4.3.

3.1.3 Chosen quantities in the different buses

Solving the power flow problem requires set quantities at different buses. The four changing variables are:

- P_i - The real power will be set at all the buses (i). This will reflect the power demand at all buses; the power generated at all the generators and the import and export of power.
- Q_i - The reactive power at bus i, consumed or generated. Reactive power will not typically be demanded by the buses, but it will be possible to set the reactive power consumption based on the reactive components, see section 2.2.4.
- Vi - The voltage magnitude at bus i. Can be determined at generators with voltage control [14, 34].
- δ_i - The voltage angle. This will not be set at any of the buses, except one, the slack bus (explained in next paragraph).

For each bus, two variables will be quantified (since there are two equations for each bus). This is done according to different characteristics for each bus, based on the following [12]:

1. Load buses ($P - Q$ buses): In load buses, the both the real - and reactive power is set. The real power comes from the demand at the bus and is determined by the actual power demand in the area. The reactive power however is not as intuitive; this will be based on historical records, load forecasts, or measurement history. Or often in practice only by the real power and a power factor (see section 2.2.1) of 0.85 or higher.

2. Voltage-controlled buses ($P - V$ buses): These buses are typically generator buses with automatic voltage control. The real power is still known, this is the power generated by the generators. The voltage magnitude will also be known due to the setpoint for automatic voltage control.

3. Slack bus ($V - \delta$ buses): This will only be one bus in the power system. This bus serves as a angle reference for all the other buses, i.e. the voltage angle will, typically, be set to zero, $\delta_{slack} = 0$, although the actual numeric value will be of no difference due to the fact that the power calculations depend only on the differences between the angles, not the absolute values. The other variable set at the slack bus will be the voltage magnitude. Neither of the power variables will be set at the slack bus, due to the total power in the system both at the buses and the lines (as described in equations (3.1.6) and (3.1.7)). The slack bus is required to "fulfill" the remaining power consumption or generation.

Chapter 4

Problem formulation

In any optimization problem, the problem formulation is often the most demanding part and is absolutely essential to achieve a solution that is reliable in the physical system. This also applies to non-physical systems such as economic and biological system [39, 44].

As in all mathematical models, the problem formulation of a physical system is usually approximation of the real world and do not require the exact characteristics as the actual system. However, using a model that is not in close relation to the real world will give the optimization no, or very little, value. As in most optimization schemes, the objective of the voltage control problem is to minimize the costs of the power transmission (such as buying new, or fixing, control components, see section 2.2.4) and to maximize the income, or utilization of the power transmitted, as well as freeing time for the personnel operating the power system, see section 2.2.2.

4.1 High voltage optimization problem

The model presented in [14] is to be used as the model and framework for the optimization. Due to the nonlinear characteristics of the power flow model, nonlinear programming is utilized. The reactive components described in [14], will be used to control the voltage level to its desired

values. Most of these are on/off components, except for some SVCs.

The problem will be presented in two ways, first by using only the discrete/integer decision variables, that means excluding the SVCs from the system. On/off components are currently the only decisions available to an operator performing voltage control (besides changing the setpoint for a SVC, but this automatically handles voltage control, see section 4.7.1).

Later the SVCs will be included in the problem formulation, as these are an important part of the voltage control performed today, see section 4.7. This will give the controller algorithm the possibility to optimize over all point discussed in section 2.2.

The MINLP voltage control problem is formulated as follows:

$$
\begin{aligned}
\underset{Q_i \in \mathbb{Z}^n}{\text{minimize}} \quad & w_V \sum_{i=1}^{N} (\epsilon_i)^2 + w_Q \sum_{i=1}^{N} (Q_{switch,i})^2 + w_{comp} \sum_{i=1}^{N} (Q_i)^2 \\
\text{subject to } & P_i = V_i^2 G_{ii} + \sum_{j=1;j\neq i}^{N} V_i V_j \left[B_{ij} sin\ (\delta_i - \delta_j) + G_{ij} cos\ (\delta_i - \delta_j) \right] \\
& Q_i = -V_i^2 B_{ii} + \sum_{j=1;j\neq i}^{N} V_i V_j \left[G_{ij} sin\ (\delta_i - \delta_j) - B_{ij} cos\ (\delta_i - \delta_j) \right] \\
& Q_{switch,i} = Q_{previous,i} - Q_i \\
& Q_{min} \leq Q_i \leq Q_{max} \\
& -\epsilon_i + V_i \geq V_{min} \\
& \epsilon_i + V_i \leq V_{max} \\
& -\pi \leq \delta_i \leq \pi \\
& P_i = P_{demand},\ \forall\ i \neq slack\ bus \\
& V_N = 1 \\
& \delta_N = 0 \\
& i = 1, \ldots, N
\end{aligned}
\tag{4.1.1}
$$

Where P_i is the real power demand at buss i, further mentioned in section 3.1 and in [14]. Q_i is the reactive power generated and consumed in each bus, which will also serve as the decision variables. *Slack bus*[1] indicate slack buses, which serve as generators that covers the surplus of power needed, the power demands for these buses will therefore not be predetermined (see section 3.1). $Q_{previous,i}$ indicates the Q_i value of bus i at the previous timestep.

V_i and δ_i are the voltage level and phase angle, respectively. G and B are the real and reactive part of the admittance matrix Y, see section 4.3.1. V_{min} and V_{max} are the voltage limits, see section 4.2.1. ϵ_i is a deviation variable for the voltage limits, this is further explained in section 4.2.1.

N are the number of buses in the network, and bus number N one of the slack buses and the bus that sets the reference voltage. w_V, w_Q and w_{comp} are cost function weights (see section 4.2.4).

Note that Per-unit calculations are used in throughout the network, hence the numeric voltage level of the slack bus, $V_k = 1$. Details on Per-unit calculations can be found in the appendix, see section A.2.

4.2 Cost function

The cost function of the problem formulation is set up to minimize the deviations from the voltage limits, and to minimize the number of control actions performed, i.e. connections of a reactor or capacitor battery (see section 2.2.4). A later addition to the cost function, which will not complicate the matter severely, is to add the SVC usage in the cost function. As mentioned in section 2.2.4, the SVC will ideally produce or consume no reactive power, this is in order to avoid saturation in case of large voltage changes.

As referred to in section 2.3.1, the cost function is in this case, as in most optimization problems, a simplification to maximize the economic,

[1] This name unfortunate since slacks in optimization theory [23] and in power system analysis [12, 19] are two different things, however slack variables in optimization theory will not be a major part of this paper.

environmental and safety requirements for the voltage control problem.

4.2.1 Voltage limits

The voltage control problem is based on keeping the voltage levels within certain given limits:

$$\begin{aligned} V_{min} &= 280kV \\ V_{max} &= 300kV \end{aligned} \tag{4.2.1}$$

For the $300kV$-lines, and

$$\begin{aligned} V_{min} &= 400kV \\ V_{max} &= 420kV \end{aligned} \tag{4.2.2}$$

For the $420kV$-lines [37].

However, instead of using strict limits, i.e. setting the voltage limits as two inequality constraints for each bus. A relaxed version of the concept soft constraints is used, see [20]. In practice this means the voltage limits can be exceeded, but at an additional cost. This is both convenient and necessary, because the number of capacitor batteries or reactors at certain buses may not be sufficient at extreme conditions, and continuous switching at boundary conditions may cause more wear and tear than necessary [37].

The mathematical way of solving this is to implement a deviation variable that will represent the distance from acceptable voltage values. As seen in the problem formulation in (4.1.1), this variable is denoted by ϵ. Recognizing ϵ in the cost function, an increasing ϵ will lead to a quadratic increase in the cost function, i.e. a large violation of the voltage limits will give high cost as illustrated in figure 4.1.

4.2.2 Reactive component switching

In addition to keeping the voltage boundaries, the cost function grows with increased switching of on/off reactive components. As mentioned in sec-

tion 2.2.2, frequent switching of reactive components decreases their lifetime severely, and will ultimately lead to increased downtime and maintenance.

Maintaining the balance between keeping the voltage limits and limiting the controller actions executed is the key to maximize the profits and environmental gain of the voltage control problem.

The part of the cost function that represents the reactive switching is denoted by Q_{switch}. Q_{switch} is an integer value and represents the number of reactive components coupled from one time step to the next.

A linear increase in couplings at one bus will give a quadratic increase to the cost function. This will both help spreading couplings to different buses, keeping the same buses from coupling all its reactive components, i.e. saturation the controller. Even more notably it helps keep the cost function smooth and thereby avoid possible problems around a non-smooth

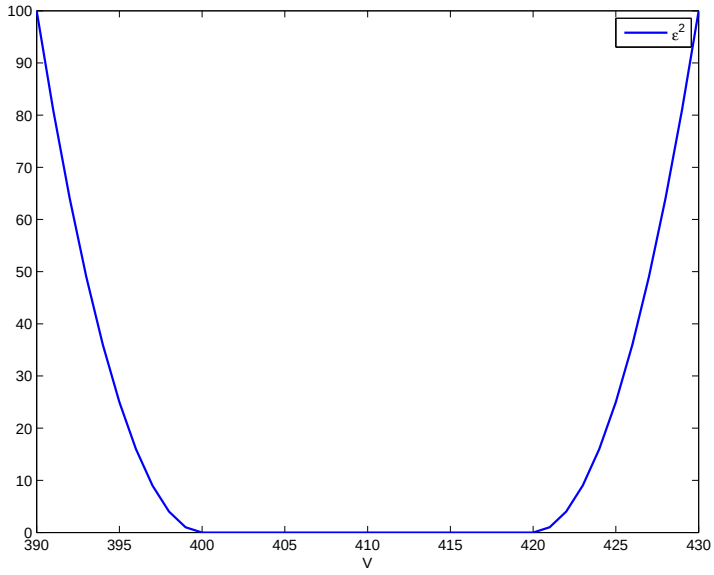

Figure 4.1: Cost of ϵ, exceeded voltage limit

zero value [23]. Examples of a smooth and a non-smooth objective function can be found in figure 4.2.

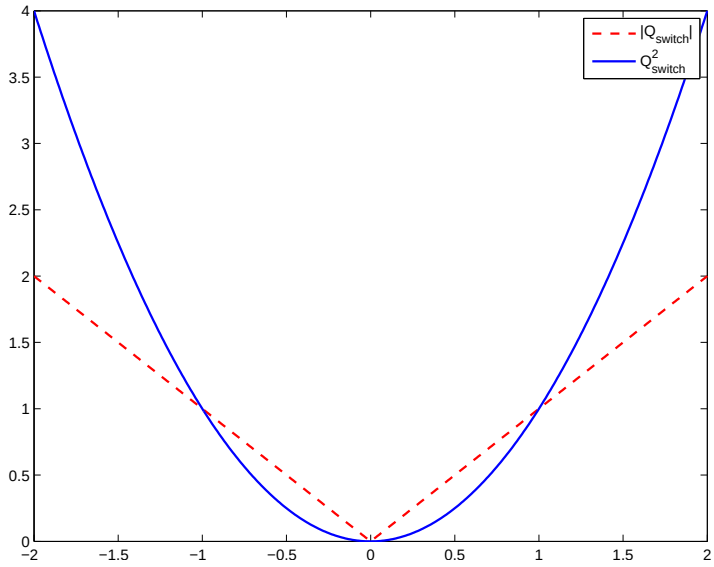

Figure 4.2: Cost of Q_{switch}, smooth and non-smooth function

One could argue that two switches in one bus should not be penalized more than one switch in two buses, and thereby a linear objective should be used. Even so, given the aforementioned qualities a quadratic cost gives the algorithm, it is still elected to do so.

4.2.3 Cost of competing components

The third part of the cost function is a cost for excessive usage of reactive components. This part is both to limit the use of a component that is not necessary and to avoid the usage of two competing components in neighboring buses, e.g. a reactor in one bus would use all the reactive power produced by a capacitor in the next.

This part also makes sure that it is a better choice to switch off a capacitor or a reactor than to switch one on.

4.2.4 Weighting

In addition to the cost function growing with the physical alterations in terms of voltage changes and reactive component switching, the cost function is also affected by the choices made for weights in the optimization problem.

Scaling the weights is vital to achieve the desired response for the optimization algorithm. A worst case scenario would be to completely disregard changes in the voltage levels because the cost of switching and use of reactive components where set too high. More on tuning these weight can be found in section 4.8.

4.3 Network model

The detailed mathematical model of the simplified high voltage network is described in [14]. However, a run-through of the most important points will also be presented in this paper.

As described in section 4.1, the basis for keeping the optimization problem within physical bounds of the optimization is the power flow model (for background theory, see section 3.1). The power flow model is based on the simplified network which is presented graphically in figure 4.6 at the end of the chapter. Each bus will also be given a short introduction, as the characteristics are described in table 4.1. The buses are also given describing names to give the reader, if familiar with Norwegian geography, some sense of distance and terrain, i.e. mountainous areas and large cities. Each bus in this system model will represent a cluster of buses in close proximity to the modeled bus. While this will not give an accurate model of the Southern Norwegian power grid, this is done to keep the number of buses at an acceptable level while exploring the usage of MINLP in a voltage control algorithm.

Bus	Number	Characteristics
Vest Agder	1	Located at the south-west tip of Norway. The entry point of the NorNed cable (Norway - The Netherlands).
Aust Agder	2	At the southern tip of Norway. The entry point for the Skagerrak cables.
Vestfold	3	At the west side of the Oslo fjord. A consumer.
Østfold	4	At the east side of the Oslo fjord. A consumer.
Oslo	5	Located in the city of Oslo. Norway's biggest city, therefore one of the more heavy consumers of electric power.
Drammen	6	Located in the city of Drammen. A large city just west of Oslo, also a heavy consumer.
Oppland(G)	7	A generator bus, located north west of Oslo, in the mountains.
Oppland North	8	Situated close to the border of the Central Norwegian Region. A consumer.
Hardanger(G)	9	A large power plant in a Norwegian scale, i.e. a generator bus, located at the end of the Hardanger fjord.
Sogn og Fjordane	10	Consumer, at the end of the Sognefjord.

Sogn og Fjordane(G)	11	Generator, just outside Førde in Western Norway.
Bergen	12	Consumer in the city of Bergen, Norway's second biggest city.
Hordaland South	13	Consumer, south of Bergen.
Rogaland North(G)	14	Generator, north of Stavanger.
Stavanger	15	Located in the city of Stavanger, Norway's fourth biggest city (third biggest in the Southern Norwegian region).
Rogaland South(G)	16	Generator, south-west in Norway.

Table 4.1: Overview of all buses in the network

4.3.1 Admittance matrix

The buses, and the distance between them (which can be found in appendix A.3) is basis for the admittance matrix of the power system. The admittance matrix consists of diagonal and off-diagonal elements. The off-diagonal elements represents the connection between two buses, if the value of the element is zero, there are no power line between the two buses. The diagonal elements of the admittance matrix are all non-zero elements, these represents the nodal admittance of the buses. The nodal admittance is affected by connecting lines, transformers, generators etc.

π-equivalents

A common simplification in the mathematical modeling of physical systems is using an existing known model. A power line is commonly modeled as a π-equivalent, the characteristic name is derived from the model sketch with a striking resemblance to the Greek letter π, see figure 4.3.

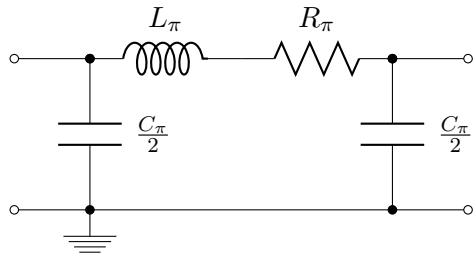

Figure 4.3: π-equivalent

The π-equivalent represents a power line with one ohmic resistance and one inductor in a series connection, and one capacitor shunt connected (in parallel) to each bus (i.e. two capacitors in total). All the variables are dependent on the line lengths and the type of power line (the type of power line used is discussed in section 4.9.1). In high voltage systems the ohmic resistances are small, and reactive losses will play a bigger part. By connecting all the π-equivalent models, the admittance matrix is generated, giving a basis for the power flow model. For more a detailed derivation of the admittance model and the system network, see [14].

4.3.2 Power flow

In the optimization problem, the power flow equations represent the connection between the physical values in the network. In section 3.1 the classic power flow model is presented.

However, the power flow model utilized in the optimal control algorithms differs from the classic power flow model in two ways:

1. The use of two slack buses.

2. The reactive power values are set according to the voltage levels iteratively, i.e. the reactive power flows are optimized on the voltage levels.

The first deviation makes it possible to choose all the reactive power in the power system (given the simplifications made in section 4.9.2), i.e. the decision variables applies for all buses. The second point is the nature of an optimization; "what is the best choice of Q_i?"

- P_i, the power demand is set at all buses, except two slack buses.
- Q_i, is determined by the optimizer at all buses
- V_i, the voltage level is set at *one* slack bus.
- δ_i, the voltage angle is set at *one* slack bus.

This will still make it possible to determined the power flow, since the number of known - and optimized variables are $2N$ (where N is the number of buses) the same as the number of equations.

4.3.3 Modifying the network model for a decentralized controller

The MINLP formulation will also be tested as part of a distributed controller algorithm. Buses in the simplified model will no longer represent clusters of buses, but buses in a part of the grid. By controlling multiple parts of the network by an MINLP in each decoupled zone, a control scheme similar to the one used in France can be explored [17, 29]. More on the decentralized model can be found in section 5.5.

4.4 Constraints

The constraints in the problem formulation contains the power flow equations, power demands and the slack bus voltage, as well as the restrictions in number of reactors and capacitors. As opposed to the voltage limits, these are hard constraints meaning these cannot be broken due to physical limitations, e.g. the number of reactive components used cannot exceed the number available. The δ_i values are also given constraints, containing them to not exceed a phase lag or lead of more than π radians or 180^o, which is also as much as mathematical possible (meaning a phase angle of for example 2π radians would in reality mean 0, since $sin(0) = sin(2\pi)$ and $cos(0) = cos(2\pi)$).

4.5 Decision variables

In conventional power system analysis [12, 19] an on/off reactive component (see section 2.2.4) as a shunt connected inductor or capacitor is used. Modeling wise, this means adding another reactive component in shunt to the capacitor in the π-equivalent, see figures 4.4 and 4.5.

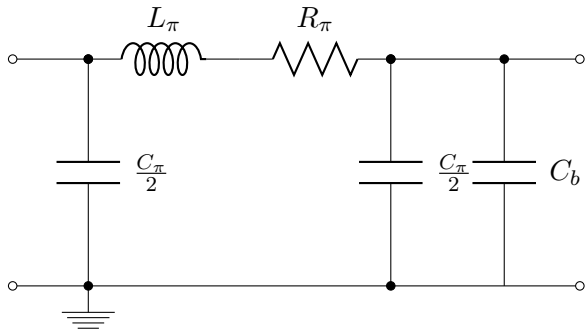

Figure 4.4: π-equivalent with connected capacitor battery

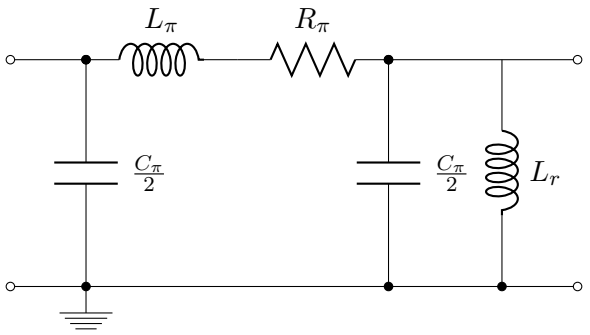

Figure 4.5: π-equivalent with connected reactor

Utilizing this model will alter the admittance matrix of the network when a reactor or capacitor is connected to change the voltage level.

However, the admittance matrix is modeled in MATLAB, and the optimization problem is written in AMPL and solved with BONMIN (for further information see chapter 5). This would lead to a continuous connection that relies on getting new admittance matrices from MATLAB via AMPL to BONMIN, which will both increase the complexity of the optimization problem and by that expose it to more sources of error, as well as severely increase the computational time.

[14] shows that a connection of a reactive component can be modeled both as an alteration of the admittance matrix and as a change in reactive power demand in the power flow equations. Given that the reactive power demands are changed in AMPL, these are chosen as the decision variables, despite it being against conventional power system analysis.

4.6 Controller dynamics

As will be discussed in section 4.10 the control algorithm is considered to be slow and non-stabilizing (i.e. a steady-state controller). It was chosen to run the controller as a new optimization for each time instance (as opposed

to MPC, LQC etc. [20]). Even so, there are some dynamic effects in the controller. Using the previous number of reactors or capacitors coupled, the controller makes sure drastic changes from one time instance to the next leads to a high cost.

$$Q_i(k-1) = Q_{prev,i}(k) \tag{4.6.1}$$

Where k is a discrete time variable and i is the given bus.

4.7 Expanding the optimization problem

4.7.1 Including the continuous control components

While the main focus of this thesis has been to incorporate the control algorithm with the discrete reactive components, the possibility for including continuous components, as for example FACTS (see section 2.2.4), will not cause major alterations to the problem formulation in equation (4.1.1). The cost function will be changed to the following:

$$\begin{aligned} \underset{Q_i \in \mathbb{Z}^n, \mathbf{Q_{SVC,i}} \in \mathbb{R}^{\mathbf{n}}}{\text{minimize}} \quad & w_V \sum_{i=1}^{N} (\epsilon_i)^2 + w_Q \sum_{i=1}^{N} (Q_{switch,i})^2 \\ & + w_{comp} \sum_{i=1}^{N} (Q_i)^2 + \mathbf{w_{SVC}} \sum_{\mathbf{i=1}}^{\mathbf{N}} (\mathbf{0} - \mathbf{Q_{SVC,i}})^{\mathbf{2}} \end{aligned} \tag{4.7.1}$$

Where the changes has been emphasized. Note that SVC costs are also model quadratic, as voltage violations, and reactor and capacitor switching and usage. This is both to ensure smoothness around zero, and because the usage of SVC ideally lies far from its extreme values, see section 2.2.2. Note also the peculiar notation of $(0 - Q_{SVC})^2 = Q_{SVC}^2$, this is to illustrate that the ideal SVC reactive power generation or consumption is 0, it will however not change on the optimization[2].

[2] Using this notation also gives the possibility to penalize deviations from a value $\neq 0$, by changing the numeric value.

By including the SVCs the reactive power part of the power flow equations also changes slightly:

$$\begin{aligned}(Q_i + \mathbf{Q_{SVC,i}}) &= -V_i^2 B_{ii} \\ &+ \sum_{j=1;j\neq i}^{N} V_i V_j \left[G_{ij} sin\ (\delta_i - \delta_j) - B_{ij} cos\ (\delta_i - \delta_j)\right]\end{aligned} \tag{4.7.2}$$

Where $(Q_i + \mathbf{Q_{SVC,i}})$ is the total reactive power produced at bus i.

There will also be added constraints on the bounds of the SVC,

$$Q_{SVC,min,i} \leq Q_{SVC,i} \leq Q_{SVC,max,i} \tag{4.7.3}$$

Where $Q_{SVC,min,i}$ and $Q_{SVC,max,i}$ are the maximum amount of reactive power the SVC are able to absorb or deliver in bus i, respectively.

As seen in the expanded cost function (4.7.1), usage of SVC reactive power will give an increased cost regardless of the reactive power used in last iteration.

Equation (4.7.2) differs from the SVCs in the actual network. SVCs are automatic components in the sense that they do not deliver a fixed, or operator determined, amount of reactive power, but takes a voltage level set point and delivers reactive power according to this (see section 2.2.4). Even so, modeling the SVCs this way gives a deterministic value for the SVCs that let the optimization program handle both types of reactive components.

The actual physical practice and implementation of the SVCs will not differ severely from the model in the sense that the reactive power generated or absorbed by the SVCs will be controlled to give the optimal voltage level, i.e. the voltage that will give minimum cost in the optimization. This means the reactive power delivered using the optimal control algorithm and using the SVC control algorithm will be of the same order of magnitude. The major difference that can be incorporated in an actual implementation is to measure the current reactive power usage by SVCs and put these measurements in the cost function instead of a decision variable. For more on the implementation and application of the controller, see section 9.3.

SVC Weight

The weight of the SVC cost will be set according to the other weight in the objective function, discussed in section 4.2.4. The most important considerations are to keep the weight high enough so that switching is preferred over SVC usage and low enough so the voltage level is still controlled.

4.8 Controller tuning

As other control algorithms, the optimal voltage controller needs to be tuned. The tuning parameters of the MINLP are the objective function weights, starting values and possibly some termination criteria, i.e. the possibility to stop at an iteration if the runtime exceeds a value or other specification is met, see section 5.2.1.

The weight needs to be set according to the economic gain of the cost function. This means finding out how much a slight violation of the voltage limits costs in comparison with the wear and tear of a switch in a reactive component, and how much the safety of a SVC with full potential is worth.

This is a study of its own, and while the weights set in this thesis will not be well tuned, they will make sure the weights are in an order of magnitude so that the controller works its desired way.

The weight for component switching will be set large enough so a switch will not be performed unless it moves the voltage levels closer to its acceptable area. It will also be set small enough to ensure voltage control is the top priority.

The weight for competing components will be kept small. This is an even lower priority than the switching criteria, as a high weight could discard cost of switching off reactive components and cause excessive switching. For more on goal programming and prioritized objective functions see [39].

The starting values and termination criteria will be addressed in section 5.2.1.

4.9 Physical simplifications

The system model has some obvious simplification, in addition to the aforementioned π-equivalents (see section 4.3.1) and number of buses in the network, all geographical distances are approximate numbers as opposed to real power line lengths. However, some physical simplifications are less obvious and should be addressed.

4.9.1 Choice of power lines

The model has been based on using only one type of transmission line, for both traditional overhead lines, and for the sea cables.

This simplification for the sea cables would essentially be unacceptable, because the capacitive characteristics of a sea cable is vastly different than an overhead transmission line, for more details on sea cable characteristics see [4]. All the same, the simplification is done because the capacitive effects of the sea cable is compensated for by designated automatic reactive components, i.e. FACTS (see section 2.2.4). This makes the overall characteristics similar to the overhead lines, and special care is not necessary.

The transmission line used is a $420kV$ duplex line called "Grackle". This has a characteristic series impedance of $0.02 + j0.32\,\Omega/km$. The capacitance of the line is $11nF/km$. Although Statnett uses a number of different lines, the characteristics are similar. Using only one type seems to be an acceptable simplification[3].

Nevertheless, the choice of using only $420kV$ lines, as opposed to both 300 and $420kV$ will affect the model severely. The characteristics of a $300kV$ line is different. However the biggest difference is the mere fact that transmitting electrical power at 300 kV affects the power in terms of resistive - and reactive effects on the power. A $300kV$ line will have larger losses, and thereby larger voltage fluctuations than a $420kV$, see section 2.2.1.

Another effect closely connected to the $300kV$ lines is the autotransformers needed to transform the power from one voltage level to another.

[3]These values are based in line parameters for power lines used by Statnett.

These also impose impedance, which leads to more power losses, both reactive and real.

Excluding the $300kV$ lines and the autotransformers will therefore make an impact on the model, at least quantitatively. The qualitative behavior of a $300kV$ line is the same as for a $420kV$ line, although the losses are greater. Therefore, it is chosen to use only $420kV$, because this will simplify the control scheme, and focus on the essential task.

It can also be argued the spatial distances between the power buses will be much larger than in a real network, due to the limited number of buses, this will lead to greater losses than short distances and therefore compensate some of the effects of only using $420kV$ lines.

4.9.2 Reactive power from other electric components

All electrical components in an AC power grid will affect the reactive power flow of a system. This includes, but is not limited to, generators, transformers and harmonic filters. This will therefore affect the voltage level throughout the power grid. The problem with this reactive power is that it is fairly unpredictable. For example, the generators produce a lot of reactive power, and ideally the generators could be introduced as a control output to the voltage control problem by delivering the reactive power needed to control the voltage to the ideal level, more on this in [14, 34]. Even so, the lack of AVRs (automatic voltage regulators) in the modeled generator buses will increase the voltage in these buses, especially when the production is high. This could ultimately lead to an unrealistic number of reactors coupled in generator buses. In the actual grid, these would not be needed.

Due to the fact that reactive power flows are both uncontrollable and difficult to predict from a simulation standpoint, they are considered to be zero in the control problem. This means that all the reactive power production and consumption comes from the control components included in the model.

The reactive power “demands” are currently what makes the optimization problem a integer problem. This is a characteristic that ideally should

be relaxed, because integer problems can cause increased runtime and non-convex problems (see section 2.3.2). However, including the reactive effects from other electrical components will not change this. Even though the reactive power consumed and generated at each bus will be a non-integer value, the decisions made in the optimization will remain integer (or at least discrete).

Adding the reactive effects to the current system model would not cause additional complications. Since the reactive power is measured continuously in the high voltage power grid, the measurements can easily be included.

4.10 Control theoretical considerations

The MINLP voltage controller is designed to control the steady-states of the voltage levels, i.e. the secondary level of the voltage control hierarchy, see section 2.2.3. The primary level will therefore deal with the transient phases - and extreme cases of voltage control, i.e. voltage collapse. More on voltage stability and the possibility of voltage collapse can be found in [19].

The time constant of the system is considered to be slow, as described in [14]. With a time constant of up to a minute, updates of decision variables should be done even slower to avoid instability issues. Given the runtime of the MINLP solver this will count as an advantage, as it reduces the pressure to deliver frequent solution updates.

Using a quadratic cost function to penalize the reactive switching makes control actions more conservative. This will also decrease the possiblity of destabilizing an already stabilized system as parallels can be drawn to a small controller gain in a classic control-loop, e.g. a PID-controller [36]. For this feature to be a factor, the weight w_Q for the reactive power needs to be large enough to make an impact on the cost function, see section 4.2.4.

4.11 Simplifications to the optimization problem

MINLP are known as the hardest optimization problems to solve, both in terms of computational time and in ensuring that the optimal solution

is also the global optima, see section 2.3. While relaxing one of these challenges is tempting, it has been deemed too great of a simplification to fit the real world.

Eliminating integer constraints would simplify the solution algorithm a great deal, there are numerous solvers for nonlinear programs, which can provide optimal solutions at a runtime much better than MINLP solvers, see section 2.3.3.

Most of the reactive power generated in the power grid can be varied continuously. Even so, the control components controlled by the regional operators today are the reactors and capacitor batteries, see section 2.2.2. The impact one capacitor or reactor has on the system will be too great to relax this condition to a continuous problem

A linearization of the power flow equations would also make the problem a simpler one. These equality constraints, with its nonlinear nature ensure non-convex MINLP. Due to this non-convexity, the global optima of the problem cannot be guaranteed. A linearization of these equations (derived in [14]) would convexify the problem. Even though it cannot be deemed a MILP, due to the quadratic objective function, a convex MINLP (MIQLP) is solvable to global optima with today's solvers.

In spite of these advantages, the power flow equations are highly nonlinear due to trigonometric and quadratic expressions. A linearization of these expressions is therefore considered to be a poor approximation to the already simplified network and the nonlinear power flow equations are kept.

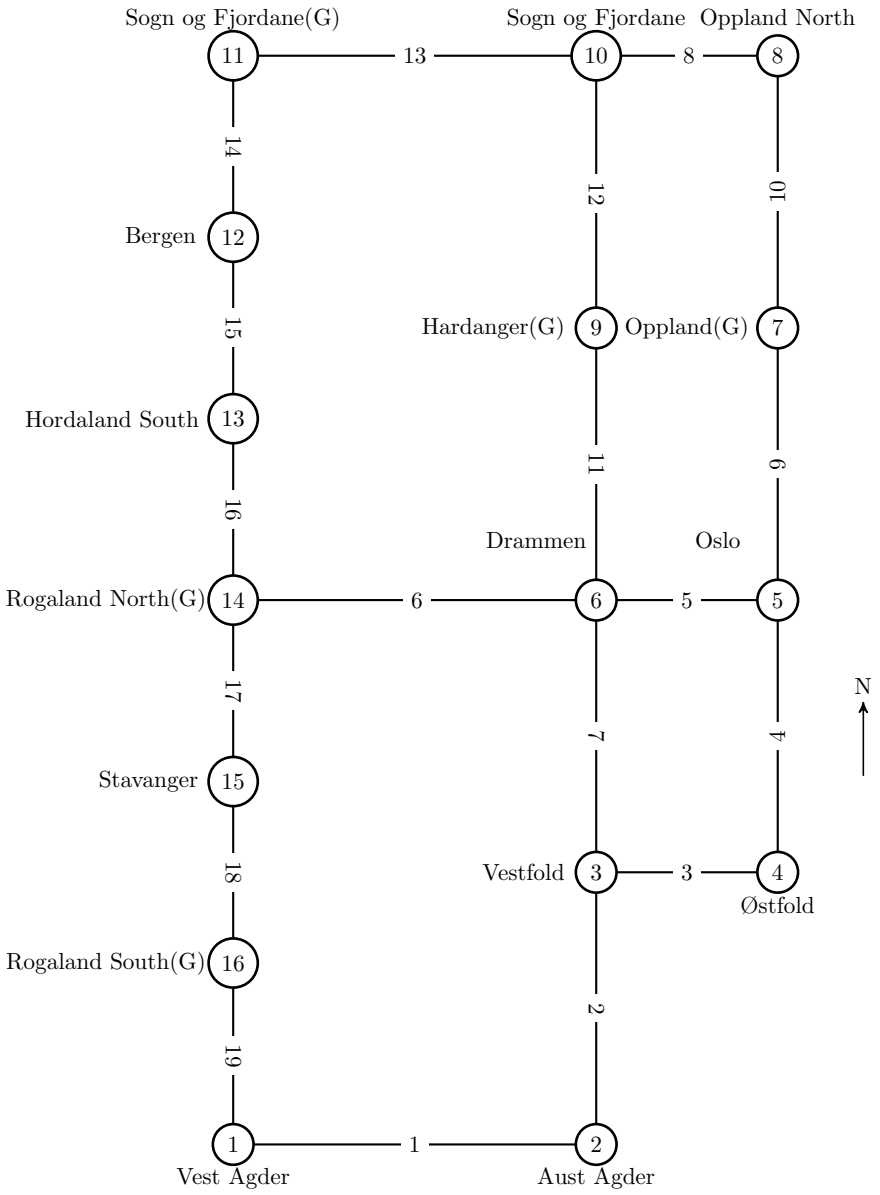

Figure 4.6: Graph of the Network, without international and interregional connections (N indicates North)

Chapter 5

Synthesis

This chapter will be a run-through of the choice of solution platform, how the control algorithm was set up, how the simulations were run and some considerations of the practical approach to the programming and simulation.

5.1 Solution platform

MINLP is a relatively unexplored field and cannot be handled by classic solvers found in MATLAB or similar mathematical modeling platforms. However strong academic communities (for example Carnegie Mellon University and IBM) are in the process of developing solvers for these problems. Most notably the BONMIN (Basic Open-source Nonlinear Mixed INteger programming) solver, distributed by COIN-OR (COmputational INfrastructure for Operations Research) [5], has reached academic recognition. BONMIN is therefore selected as a solver for the high voltage optimization problem.

5.1.1 BONMIN

BONMIN solves the mixed-integer nonlinear program using experimental open source C++ code [1].

Although exact solutions of non-convex problems can prove difficult, BONMIN provides heuristic solutions for problems with non-convex objective functions and constraints, i.e. the solutions provided by BONMIN cannot guarantee global optima for the voltage control problem [2].

The algorithm used can be varied from B-BB, a NLP branch and bound method (see section 2.3.3), B-OA, an outer approximation decomposition algorithm (see [2, 9]), B-QG, Quesada and Grossmann's Branch-and-Cut algorithm (see [2]) or B-Hyb, a hybrid between B-OA and B-QG. In the voltage control problem, B-BB is used, as recommended in most literature for non-convex problems [1].

Using the MINLP algorithms require the use of solution algorithms for NLPs and MILP, here BONMIN uses IPOPT, COIN-OR's interior point algorithm (see section 2.3.3 and [42]) and Cbc, COIN-OR's branch and cut algorithm (see section 2.3.3 and [10]), respectively. The BONMIN branch and bound is actually only an extension to the Cbc (COIN-OR branch and cut), where the LP relaxations are exchanged with NLP relaxations.

Given the uncertainty of a non-convex problem, options in BONMIN allows the solver to look for better solutions than a the lower bound of the branch and bound algorithm [7]. By allowing this, the runtime of the algorithm will fast become too great to be used in an online controller algorithm; this feature is therefore discarded in the voltage control problem. Even so, utilizing the possibility to resolve the optimization problem at different randomly chosen starting point can provide less instances of infeasible solutions, since the default value in BONMIN for resolving is zero, which again means that one infeasible starting point can give an infeasible solution and an immediate termination of the solver at the current time instance [41].

Though other solvers do exist, many of these are commercial software, and would therefore require an initial investment. More information on these can be found in [7].

5.1.2 AMPL - A modeling language for mathematical programming

The programming language used for the implementation of the control algorithm is AMPL. AMPL is a mathematical modeling language tailored for complex optimization and integer programming. The language is easy to read and write for inexperienced users and provides built in tools for arithmetic, logical, algebraic, trigonometric and conditional expressions, to name a few. While supporting multiple solvers, the AMPL language was chosen to a great extent for its compatibility with BONMIN. AMPL is commercial software, but provides student licenses free of charge. [11]

5.2 Initial conditions

A MATLAB script produces the parameters needed for the optimization, as well as the starting conditions for the variables in the optimization (the script is included in the attached CD). The parameters are set according to the system requirements and the mathematical model of the power grid. The power demands are set up in one of two ways, they are either predetermined, set according to actual Statnett data (see section 5.4.1), or randomized between given bounds, set by MATLAB (see section 5.4.2).

5.2.1 Controller tuning

As mentioned in section 4.8, tuning of a controller is vital to achieve the desired response. In the voltage control algorithm there are several tuning parameters to handle. The parameters chosen in this section are chosen with the purpose of testing the controller algorithm as a proof of concept, to see if MINLPs can be applied for voltage control. Even so, a precise tuning scheme would require a far more comprehensive study.

Weigths

The weights for the cost function is set according to the specifics in section 4.2.4. Given that the voltage levels and the power is given in *pu*-values

(scaled vaules to evaluate all components in a power system, see appendix, section A.2) the weight need to be set according to the set scaling.

The base values for the *pu*-calculations is given as follows:

$$V_{base} = 410\ kV \tag{5.2.1}$$
$$S_{base} = 100\ MVA \tag{5.2.2}$$

This means the voltage level will have an operating point around $1pu = 410\ kV$, and the bounds will be set by the limits given in equation (4.2.2) in section 4.2.1. It is therefore more natural to use a base level of $410\ kV$, which is not at the boundary condition, rather than the more obvious $420\ kV$, since the slack bus will be given the voltage value of $1pu$, see section 3.1.3.

The power base, S_{base}, is set according to the size of a reactive on/off component. This means Q_i is an integer number based on number of components coupled (negative for reactors, positive for capacitors). Given that this model handles power of the same magnitude as the real network, on fewer buses, rather large components are used to achieve sufficient control.

With these values in mind, the weights for the voltage level, SVC and the reactive switching is set. If the values were to be identical, the switch of one reactive component would cost as much as a voltage level of $840\ kV$, which is a not physically manageable in the Norwegian power grid. It is therefore very clear that $w_V \gg w_Q$ and $w_V \gg w_{SVC}$.

Also, given the same value for the SVC weight as the reactive switching would eliminate the controllers ability to switch a reactive component to free up SVC potential, see section 2.2.2. Therefore it is known that $w_{SVC} > w_Q$.

What is considered the least important optimizing task is the cost of competing components and excessive control component usage. This factor is most important at the first step of a controller series to ensure a good starting point. The w_{comp} value is therefore set low.

Experimentally the weights are set to the following values:

$$\begin{aligned} w_V &= 1 \times 10^6 \\ w_Q &= 0.1 \\ w_{comp} &= 1 \times 10^{-3} \\ w_{SVC} &= 1 \end{aligned} \tag{5.2.3}$$

Using these weights, a violation of $\approx 0.005\ kV$ will give an equivalent increase to the cost function as coupling 100 $MVAr$ in 10 of the SVCs and 10 times the cost of coupling 10 components (in different buses). This value might be excessive; however it gives the controller the desired dynamics because it will generally prioritize the voltage control as opposed to conservative component switching.

Note also that these are the weights used when the controller is running. For the initial step, the weight of controller switching will be set to zero, $w_Q = 0$, as no previous control scheme exists. The cost of competing components limits the controller from coupling an excessive number of components at the initial step.

Termination

Given that a non-convex MINLP can cause severe problems when searching for a global optimum, i.e. give infinitely large runtime, some bounds for the terminating the solver is set. BONMIN provides several options for terminating the solver at the best known solution [1]. The voltage control algorithm terminates either if the runtime exceeds 5 minutes or if the best known solution is less than $\frac{w_Q}{100}$ away from the best possible solution, see section 2.3.3 on branch and bound. This phenomenon can be expressed with the following pseudocode:

if $(cost_{bestpossible} - cost_{bestknown} < \frac{w_Q}{100}$ **or** $time \geq 5\ minutes)$ **then**
  $cost = cost_{bestpossible}$
  Terminate
end if

An exception to the rule is the initial timestep where the termination time will be set to 15 minutes instead of 5. This is to ensure a good starting condition for the controller. Which is reasonable to assume given that the controller would not experience "cold starts" when operating at a real power system.

5.2.2 Starting points

In any optimization problem, good starting points can substantially reduce the runtime. For non-convex problems, the starting points can be the difference between a global or a local solution, or even seemingly infeasible solutions.

The starting points for the voltage controller are set according to all known values to ensure usage of current knowledge. As seen from the problem formulation in equation (4.1.1), the power consumption and generation are modeled as equality constraints. Since these are known values, the starting points of all real power variables will be set to predetermined values. For the reactive power and the voltage levels, the change from one timestep to the next will not be of vast magnitude (since the change is relative to the previous timestep, see section 5.4.2) and the solutions found in previous iteration will be used. For the first timestep, default BONMIN values will be used for the reactive power and voltage variables.

5.2.3 Other requirements

BONMIN provides presolving to reduce the problem size and decrease the runtime, this does however require a substantial amount of memory and may cause stack overflows [41]. The presolver is therefore turned off, which increases the runtime of the algorithm, but not to a point where it severely affects the outcome. Using more powerful computers, this problem can be avoided. More on presolvers can be found in [23].

Some other BONMIN default settings can give unwanted features. The default value for the number of root nodes to test before terminating on an infeasible solution is 1. Increasing these values to 10 reduces the risk

of obtaining an infeasible solution. It will however increase the runtime slightly.

5.3 System specifications

The controller algorithm has some values that need to be set prior to the simulations. Throughout the Southern Norwegian power grid, the numbers and types of reactive components vary. The available compensation power (reactive power) in each bus is therefore not the same. However, as a simplification, and because this controller algorithm is meant as a proof of concept, the available reactive power in each bus will be equal. This means that the number of reactive on/off components is the same and that there will be an SVC at each bus.

Modeling the system with SVCs at all buses seem excessive, however the number of continuous control components in the Southern Norwegian power grid exceeds the number of buses in the model and the system is tested with the same power levels, see section 5.4. [37]

The number of reactive on/off components and SVC limits are set as follows:

$$\begin{aligned} Q_{min} &= -5pu \\ Q_{max} &= 7pu \\ Q_{SVC,min} &= -2pu \\ Q_{SVC,max} &= 2pu \end{aligned} \tag{5.3.1}$$

Where the notation can be recognized in the problem formulation in equations (4.1.1) and (4.7.3).

The values in (5.3.1) and the base values in (5.2.2), gives a reactive potential of $-500\ MVAr$ and $+700\ MVAr$ for the on/off components and $\pm 200\ MVAr$ for the SVCs.

The seemingly over excessive access to reactive power in a bus (especially capacitors [37]) compensates for long line lengths, few buses and lack of reactive power from other components, see section 4.9. This also proves

excessive in all simulations but one, see section 6.3. For further discussion on capacitor usage, see section 8.1.1.

5.4 Simulation

The simulations are run with two different methods. One is based to two case studies with power demands based on actual data acquired for the Statnett database. The other using MATLAB scripted Monte Carlo simulations to determine the power demands. Both simulation methods are based on running one case study over several given timesteps. The starting optimization will initiate the reactive components coupled *without* increasing the cost function, and the following steps will be a result of reasonable changes in power demand compared to the starting solution.

5.4.1 Heavy - and light load case study

The power generation and consumption acquired from Statnett is based on actual numbers from eight zones around Norway, six of which is located in the Southern Norwegian region, as well as import and export. The data from these six regions including the international connections is the starting point for determining the power demands throughout the simplified network based on 16 buses.

The data logged cannot be used directly in the modeled system. The generation and consumption is divided between the buses in geographical proximity to the given region. This will give a good indication as to how the power flows change in the grid over time. As the power demands are logged each hour, the power fluctuations are generally larger than they would in a typical timestep for the running controller (about 5 minutes). This helps to test the robustness of the controller [36].

This will also lead to much greater generation and consumption in each bus than one bus will experience in the Southern Norwegian power grid.

The light load case is a summer day in July, the power consumption and generation is low due to warm weather. The data points are taken

between 0600 in the morning and 1700 in the afternoon. This gives 12 logged values to be used in the simulations and includes the morning hours which are the most important of the day, in regards to voltage control.

The heavy load case is a winter day in January. Due to cold weather the power consumption and generation is high. The heavy load case will include data points from the same hours of the data as the light load case 0600-1700.

5.4.2 Monte Carlo simulation

In addition to testing the control algorithm on two specific cases, the controller is tested on several cases with randomly selected real power at each bus (except the slack buses), at the startup, i.e. the first time instance. The randomly selected power is bound by the maximum and minimum generation or consumption of power in each bus based on the cases from section 5.4.1.

$$min(P_{case,i}) \leq P_i(0) \leq max(P_{case,i}) \tag{5.4.1}$$

Where i is the bus number, 0 indicates that it is the initial condition. The subscript *case* indicates either of the cases in section 5.4.1.

From the starting conditions the new power consumption and generation will be set according to the previous timestep. The change in one bus will be between zero and the biggest change made in one timestep in the respective bus in the cases in section 5.4.1, both in the positive and negative direction.

$$0 \leq |\Delta P_i| \leq max(P_{case,i}(k) - P_{case,i}(k-1)) \tag{5.4.2}$$

Where i is the bus number and k is the discrete timestep. The subscript *case* indicates either of the cases in section 5.4.1.

An additional requirement is that the sum of the power generation and consumption is negative. This is added due to the fact that the slack buses are regarded as strictly generator buses, i.e. $P_{slack} \geq 0$. Discarding this could lead to high power production in one slack bus, and consumption

by the other, to optimize the voltage levels. That does not reflect real life voltage control.

$$\sum_{i=1, i \neq slack}^{N} P_i \leq 0 \tag{5.4.3}$$

In equation (5.4.3), N is the number of buses and *slack* indicates one of the slack buses.

This setup will give the power grid some cases with extreme conditions, way beyond conditions met in the actual power grid. This happens both because some buses will have "winter" conditions and some "summer" conditions at the same time, and because the grid can experience extreme changes from one timestep to another. Running the control algorithm at these conditions will further test the robustness of the controller. Other simulations will present more "normal" conditions, allowing the controller to operate at day to day conditions.

5.5 MINLP in a decentralized controller

The controller algorithm can easily be used in a distributed model. The concept of the distributed controller is further explained in section 2.2.3. The basic idea is to split the power system into several decoupled zones and solving an MINLP in each zone independent of one another.

Transferring the simplified power system network into a part of the Southern Norwegian network is done by reducing the total power consumed and generated, as well at limiting the reactive power available. The model setup in figure 4.6 will remain the same. For example, a generator in the Southern Norwegian power plant will not produce more than $\approx 1000\ MW$, so trying to limit the power demands to values of this magnitude will be the basis. This means reducing the power demands lower limit by a factor of two, and the upper limit by a factor of 1.5:

$$\begin{aligned} P_{lower,cent} &= 2 \times \ P_{lower,decent} \\ P_{upper,cent} &= 1.5 \times \ P_{upper,decent} \end{aligned} \tag{5.5.1}$$

Where the subscripts *cent* and *decent* represents the centralized and decentralized model, respectively. Note also that the power demands are still randomized and only the bounds will be reduced by this factor, not necessarily the actual values. This means it is not the same reduced cases that are run for the centralized and decentralized model.

The control components available will also be limited; they will reflect realistic part of the power grid. The *pu*-value of the apparent power will receive a new value of:

$$S_{base} = 50 \ MVA \tag{5.5.2}$$

This will reduce the size of one reactor and one capacitor to 50 MVA.

There will only be given reactors and capacitors to odd number buses, i.e. bus number 1, 3, 5,..., 15. This will more accurately reflect the power system as not all buses have reactive components. The decentralized model will only be tested for the model *including* the SVCs, as the model is not thoroughly tested and will serve more as an understanding of the behavior when the power demands are low. SVCs will only be given to every fifth bus, i.e. bus number 5, 10 and 15. The bounds for reactive components on the distributed system will be as follows:

$$\begin{aligned} Q_{min}(2n+1) &= -5pu \\ Q_{max}(2n+1) &= 5pu \\ Q_{SVC,min}(5m+5) &= -2pu \\ Q_{SVC,max}(5m+5) &= 2pu \end{aligned} \tag{5.5.3}$$

Where $n = \{0, 1, ..., 7\}$ and $m = \{0, 1, 2\}$. This gives a reactive potential of $\pm 250 \ MVAr$ for the on/off components in every other bus, and $\pm 100 \ MVAr$ in every fifth bus for the SVC model.

Chapter 6

Results - Test cases

This chapter will present the results of the optimization simulations for the two predetermined test cases. These simulations will be run with the same power demands on both the model including the SVCs, see section 4.7, and the one only containing on/off components, see section 4.1. Running both controllers is necessary for two reasons:

1. Test that the controller will function by only making integer decisions.

2. Test that the controller will minimize SVC usage.

The results will give an overview of the voltage level throughout the power system, the real - and reactive power, as well as switching and SVC usage. An important note is that though the Statnett system data acquired is logged only by the hour, the timesteps in the simulations may just as well represent a 5 minute time span, since 5 minutes is the maximum runtime for any optimization, see section 5.2.1.

All the simulations will be run 11 timesteps (12 optimizations including the initial optimization). The analysis of the results will be presented in chapter 8.

6.1 Test cases

The controller algorithm will, as mentioned in section 5.4.1, be tested for two cases where the data is derived from actual Statnett data. The Statnett data is altered to fit the system model, and is included in the appendix, see section A.4.

The values presented in the two test cases will be indications as to how the controller will behave with real data; a proof of concept. Still, a quantifiable comparison to the actual power grid cannot be made as the modeled network has significantly less buses.

6.2 Light load test case

As previously mentioned the light load case study is derived from a July day in Southern Norway. The case shows how the controller would operate when the changes and total load is small.

6.2.1 System model without SVCs

Voltage levels in all the buses is shown in figure 6.1. As seen, the voltage levels stays within its bounds.

Figure 6.2 shows the number of capacitors coupled at the given timestep. As expected when the line loads are low, the need for voltage increases is small. Hence, no capacitors are coupled.

Figure 6.3 shows the number of reactors coupled at the given timestep. As seen are there are some reactors coupled at all times, as expected with a low load, which lead to Ferranti effects, i.e. the increase in voltage level [16]. When the power demand increases, the need for compensation is reduced, and some reactors are decoupled.

Comparing figures 6.3 and 6.4 shows that the number of switchings done from the previous timestep is directly a function of reactors coupled, as expected when no capacitors are used. In figure 6.4 the starting point indicates the number of reactive components coupled at the initial optimiza-

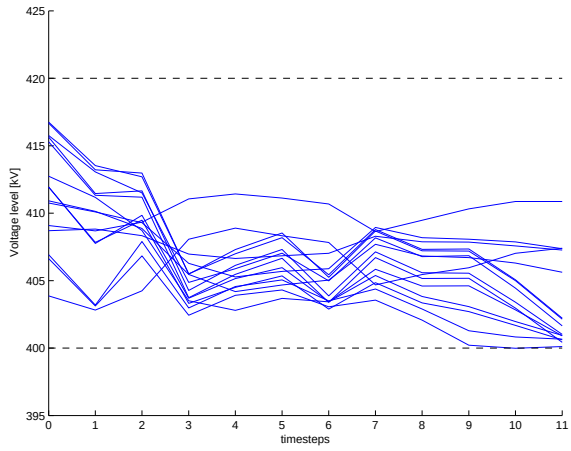

Figure 6.1: Voltage level in all buses (except the slack bus). The horizontal dashed black lines indicates the voltage limits - Light case without SVC

tion, remember that this does not impose additional cost to the objective function.

By inspecting figures 6.4 and 6.5 one can clearly observe that since the nominal voltage level are meet, the cost function is mainly a function of reactive component switching.

The total time, and which optimizations (timesteps) used the most time, can be found in figure 6.6. All the optimizations of the light case terminated before the time limit of 5 minutes (the initial timestep has 15 minutes).

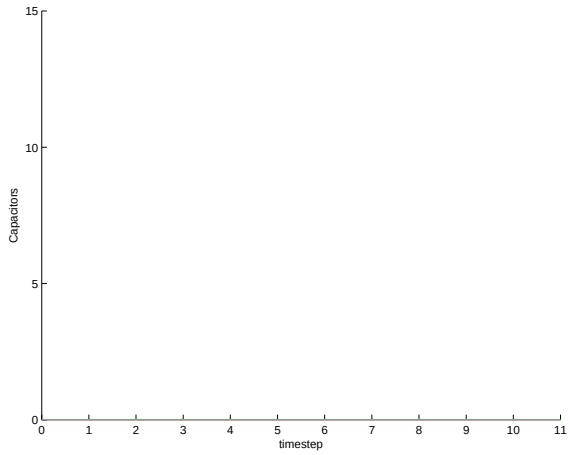

Figure 6.2: Total capacitors coupled - Light case without SVC

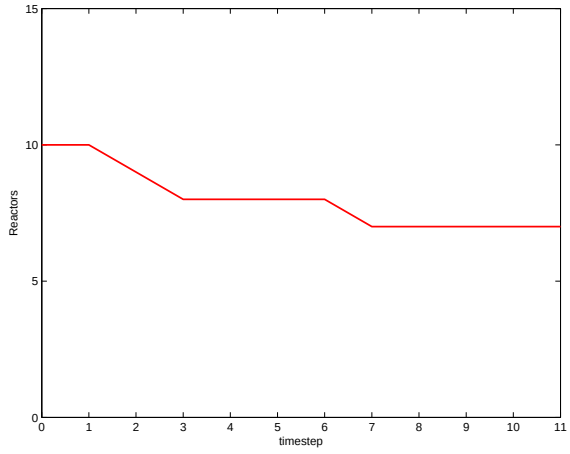

Figure 6.3: Total reactors coupled - Light case without SVC

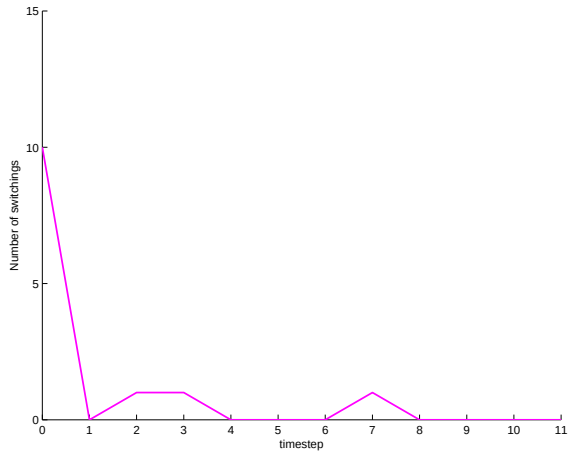

Figure 6.4: Total switching at one timestep - Light case without SVC

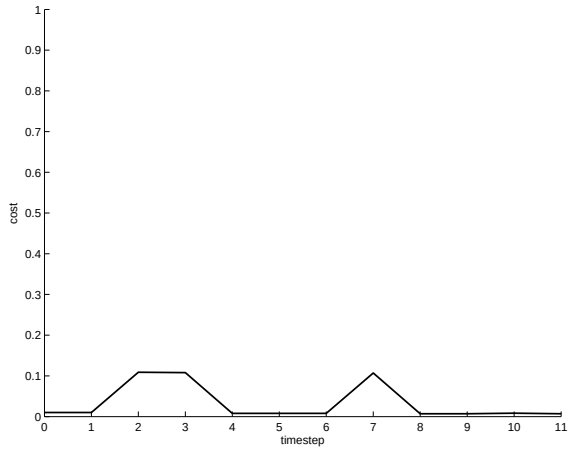

Figure 6.5: Total cost - Light case without SVC

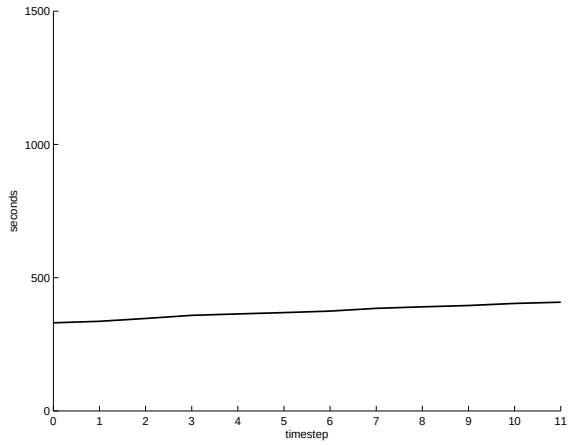

Figure 6.6: Total time elapsed - Light case without SVC

6.2.2 System model with SVCs

Utilizing the same power demands on the same system model, but including continuous decision variables does not impose major changes on the control scheme, the results can be found in figures 6.7-6.13. Note that when including continuous decision variables the total computational time was drastically reduced, see figure 6.13.

The only plot not included in the previous section is the SVC usage in figure 6.11. As seen the usage of SVCs are kept low.

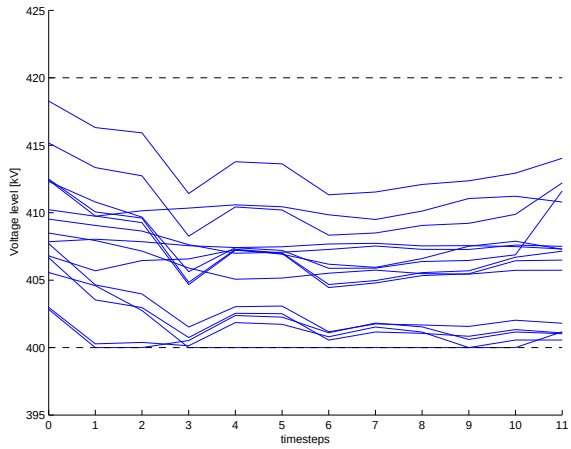

Figure 6.7: Voltage level in all buses (except the slack bus). The horizontal dashed black lines indicates the voltage limits - Light case with SVC

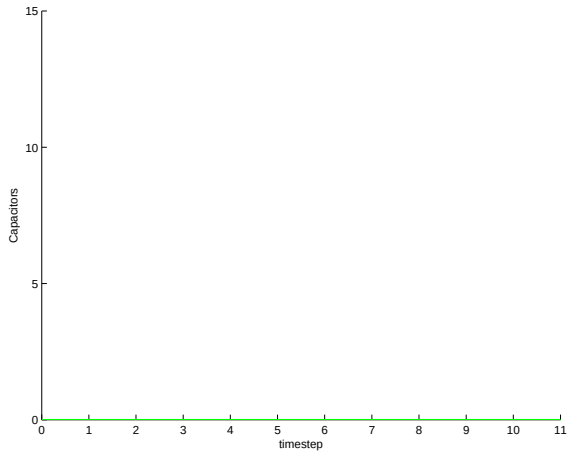

Figure 6.8: Total capacitors coupled - Light case with SVC

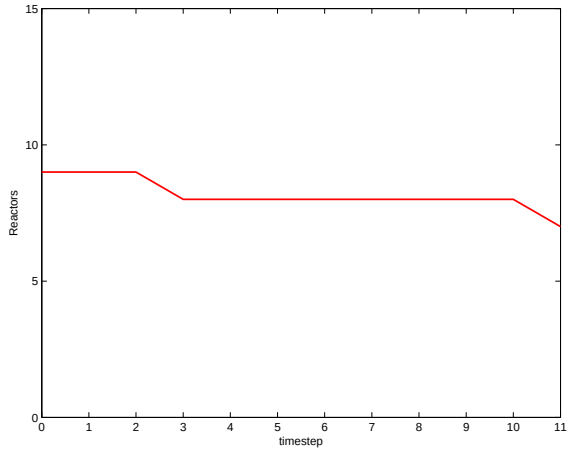

Figure 6.9: Total reactors coupled - Light case with SVC

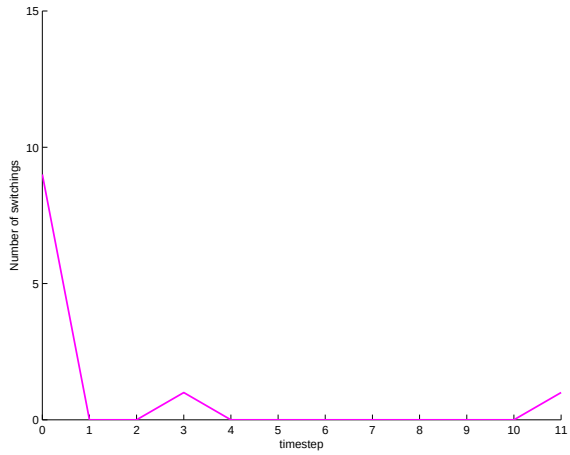

Figure 6.10: Total switching at one timestep - Light case with SVC

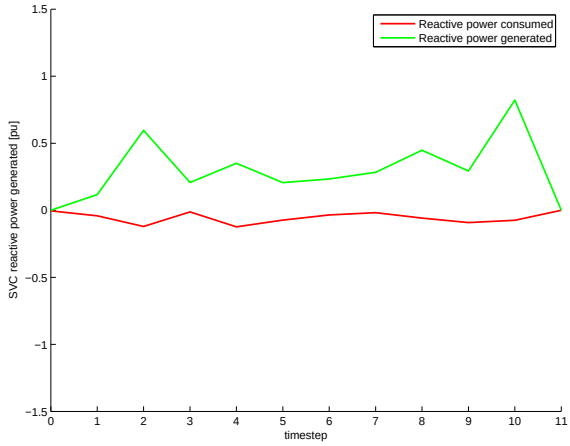

Figure 6.11: Total SVC usage in the system - Light case with SVC

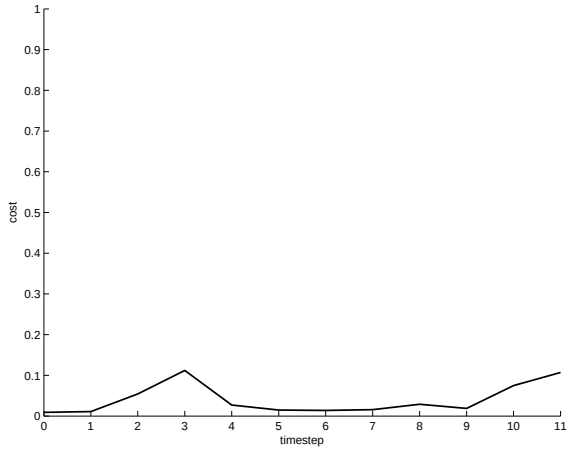

Figure 6.12: Total cost - Light case with SVC

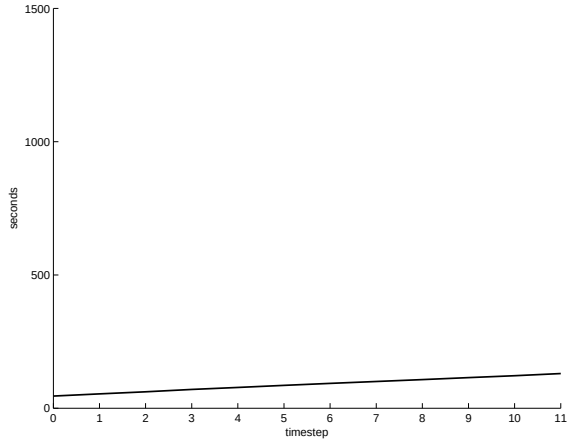

Figure 6.13: Total time elapsed - Light case with SVC

6.3 Heavy load test case

In this section, the numbers for generated and consumed power in the system are derived from a heavy loaded day. That means the generation and consumption of the entire Southern Norwegian power grid is divided between 16 buses and 19 power lines. This leads to large inductive effects on the power lines and severe voltage drops. Generator buses will experience voltage increases as there are no AVRs.

Appendix section A.4 shows the power demands and generation, notice that in some buses the generation is up to $4.5\,GW$. This is not possible in the Norwegian power grid, where the largest power plants are about $1\,GW$.

6.3.1 System model without SVCs

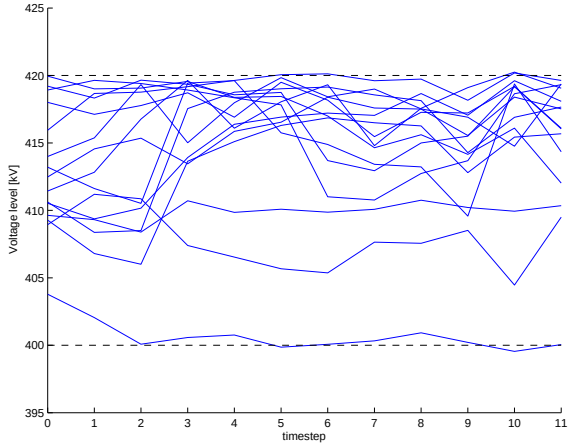

Figure 6.14: Voltage level in all buses (except the slack bus). The horizontal dashed black lines indicates the voltage limits - Heavy case without SVC

In the heavy load case study, the fluctuations of the voltage in each bus, and the variation between them, are greater than in the light case, see

figure 6.14. Notice especially that one bus lie near the low limit for the duration of the simulation, closer examination show this is bus number 6, this is further analyzed in section 8.1.1. After 10 timesteps, it can be seen that slight voltage violations has been made.

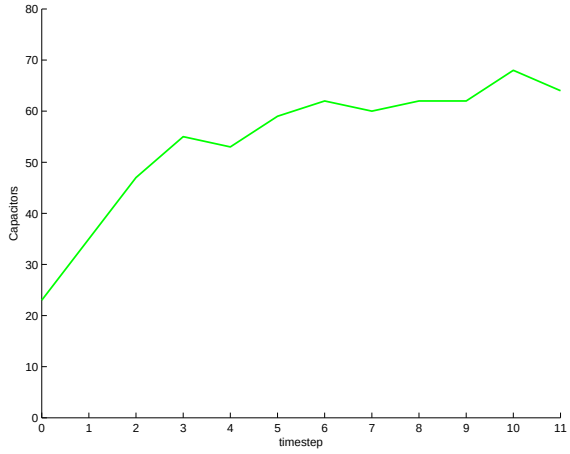

Figure 6.15: Total capacitors coupled - Heavy case without SVC

Figure 6.15 shows the total number of capacitors coupled at the given timestep. As predicted, heavy loads incites capacitor coupling.

The number of reactors coupled are displayed in figure 6.16. As expected, the reactor couplings done when the line loads are this heavy are minimal.

Figure 6.17 shows the number of switchings done from the previous timestep. In this case this is closely related to the number of capacitors coupled, $Q_{switch} = Q - Q_{prev}$, see the problem formulation (4.1.1).

The cost throughout the simulations are shown in figure 6.18. At timesteps 1, 2 and 10 there are spikes in the cost function, these are related to heavy switching (timesteps 1 and 2) and small voltage violations (timestep 10).

Despite a severely increased computational time in proportion to the

light case study, see figure 6.19. All the optimizations are terminated within the time limits.

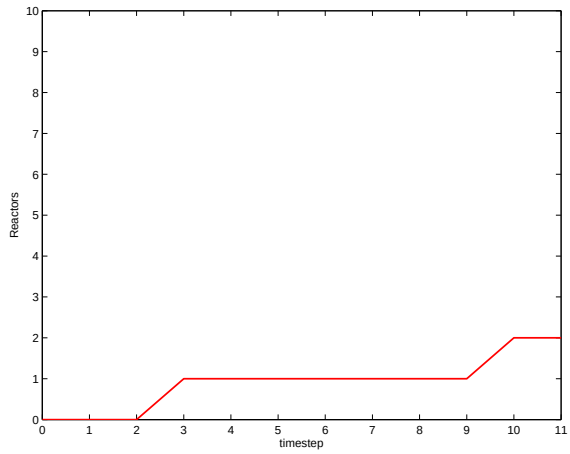

Figure 6.16: Total reactors coupled - Heavy case without SVC

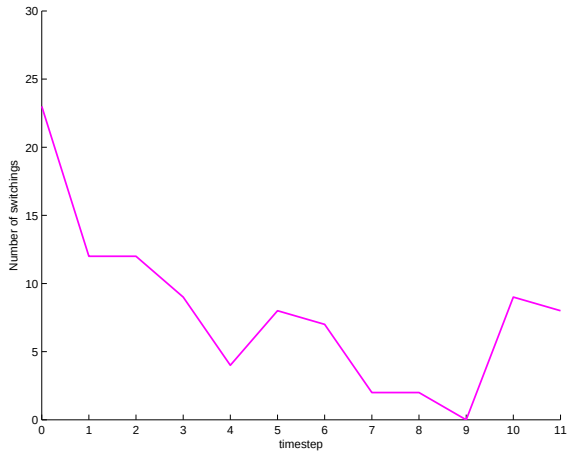

Figure 6.17: Total switching at one timestep - Heavy case without SVC

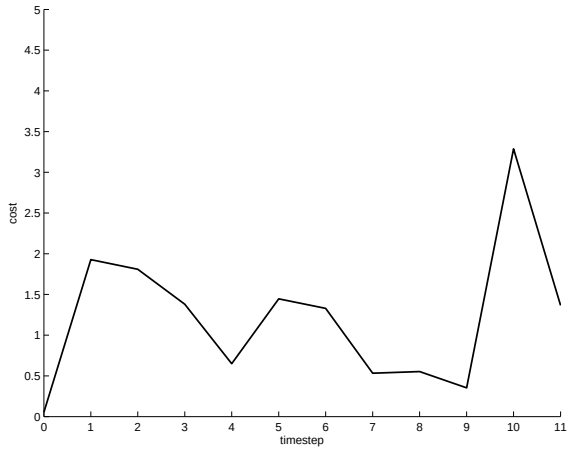

Figure 6.18: Total cost - Heavy case without SVC

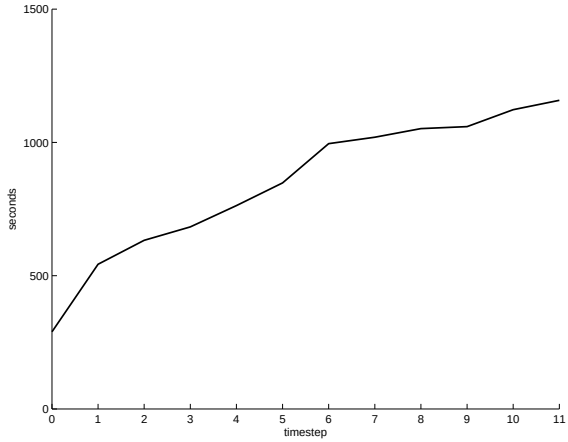

Figure 6.19: Total time elapsed - Heavy case without SVC

6.3.2 System model with SVCs

The heavy case is also simulated with the model including the SVCs. Figures 6.20-6.26 shows the results.

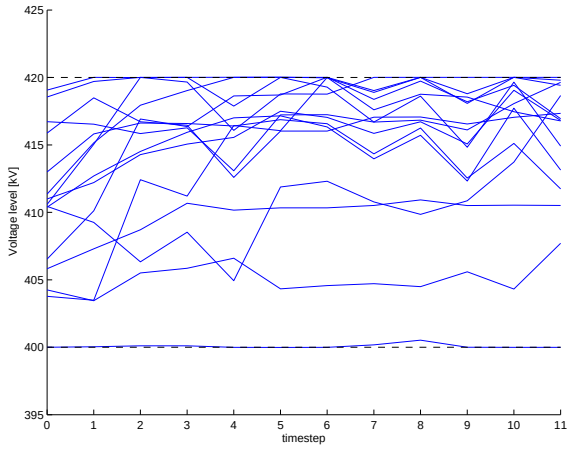

Figure 6.20: Voltage level in all buses (except the slack bus). The horizontal dashed black lines indicates the voltage limits - Heavy case with SVC

Contrary to the model without the SVCs, the voltage limits are kept for the duration of the simulation, see figure 6.20. However, the characteristics of the system remains, with low voltage levels in bus 6, and generally high voltage levels throughout the rest of the system.

Capacitor usage, see figure 6.21, is close to identical to the model without the SVCs. As are the case with reactor usage (now zero, see figure 6.22), switching (figure 6.23) and cost (figure 6.25).

As opposed to the previous model, SVC usage, displayed in figure 6.24, prevents the voltage violations after 10 timesteps. This causes the spike in the cost function, not the voltage violations as in figure 6.18. As final notion on the heavy case study; the time used when including the SVCs in the model, drastically falls.

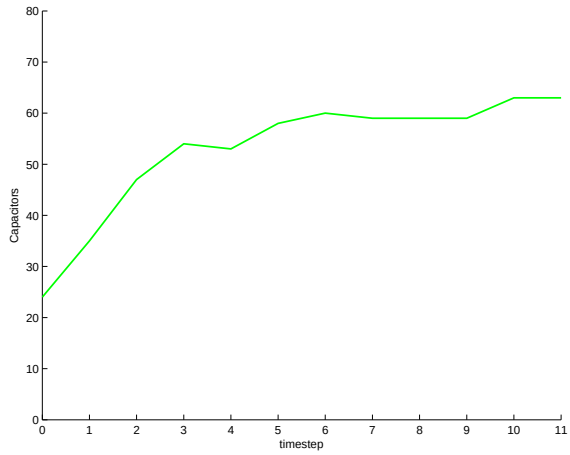

Figure 6.21: Total capacitors coupled - Heavy case with SVC

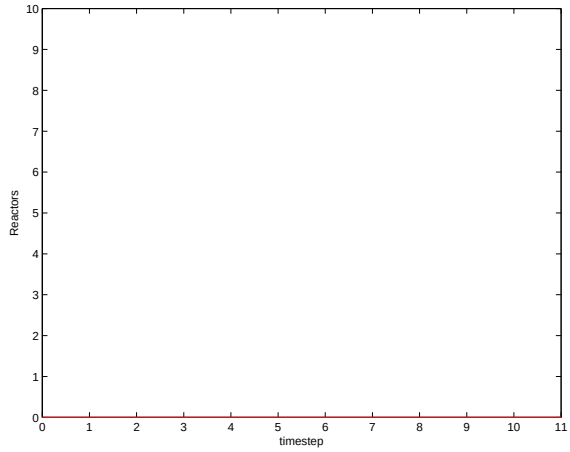

Figure 6.22: Total reactors coupled - Heavy case with SVC

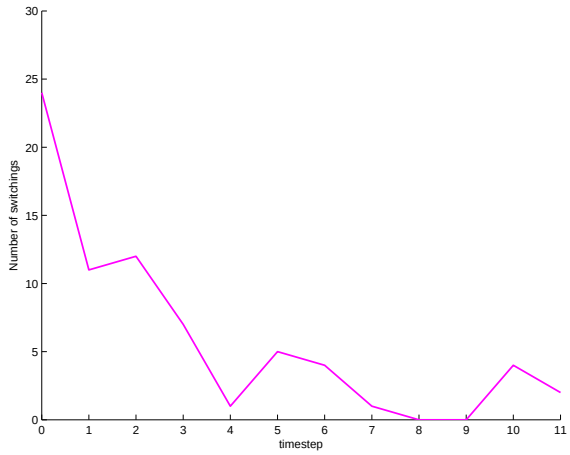

Figure 6.23: Total switching at one timestep - Heavy case with SVC

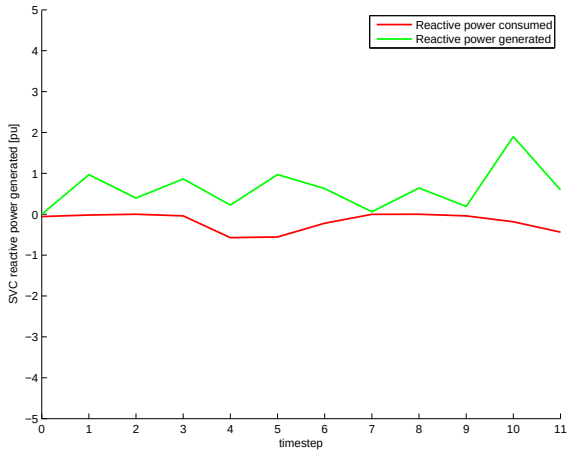

Figure 6.24: Total SVC usage in the system - Heavy case with SVC

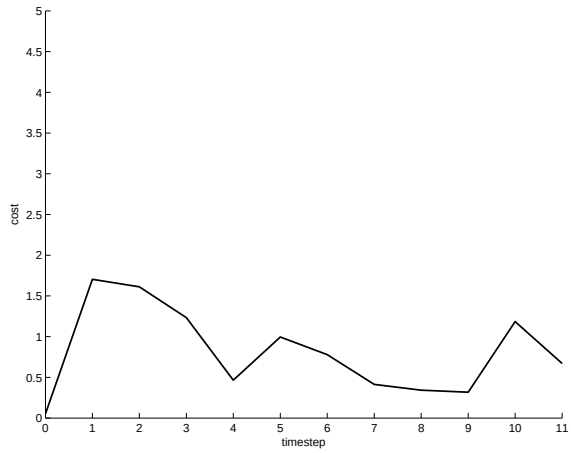

Figure 6.25: Total cost - Heavy case with SVC

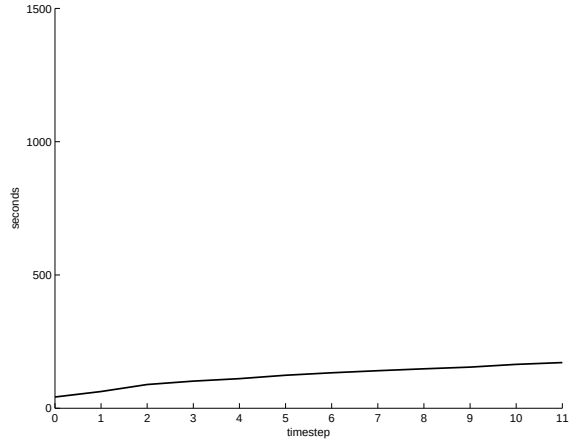

Figure 6.26: Total time elapsed - Heavy case with SVC

Chapter 7

Results - Monte Carlo simulations

This chapter will present the Monte Carlo simulations. It has been chosen to run 100 different cases for each model. These simulations will be run with the same power demands on both the model including the SVCs, see section 4.7, and the model only containing on/off components, see section 4.1. This means a total of 300 Monte Carlo cases, as the decentralized model will *only* be run with the SVCs.

All simulations run 11 timesteps plus the initial optimization, as with the predetermined cases. A more thorough analysis of the results can be found in chapter 8.

7.1 Monte Carlo simulations

The Monte Carlo simulations have too many variables to present everyone (100 cases $\times$ 16 buses $\times$ 12 timesteps = 19200 voltage levels, real - and reactive power values, switching schemes etc.). A statistical analysis of all the optimizations will therefore be presented. This will handle voltage and power statistics, computational time elapsed, total costs etc. All these statistics will be included to show how the voltage controller handle power

changes and handles different scenarios. It will also give a good indication as to whether the control algorithm is suited to handle the control problem. All the logged parameters can be found on the included CD.

Status

As the solver handle a series of different power demands at different time instances, the solution algorithm terminates in one of four possible ways:

- **Infeasible solution**, this may happen when a non-physical power demand is given to the optimizer; this can lead to negative voltages or reactive demands outside the feasibility region. Infeasible solutions did not occur during the simulations and this value will be zero in all plots.
- **Interrupted solution** is found, as mentioned in section 5.2.1, if the solution algorithm is stopped after a given runtime. All interrupted solutions have given a satisfactory solution, i.e. close to the best possible, and will be used in the statistical evaluations.
- **Optimal solution** is found if the optimizer is able to find a solution close to the best possible within the given time limit. Note again that for a MINLP this is only a heuristic solution, i.e. there is no guarantee that it is the global optimum.
- **Full memory** is the forth possible status is if the computer experiences a full memory. This is however only a problem if the presolver is switched on, as mentioned in section 5.2.3. Throughout the simulations this value will be zero, as the presolver is switched off.

Cost

The cost in each timestep will be presented as a distribution of the number of optimizations terminated at this given cost level. The cost level will be one of the following four:

- **No cost**, indicates a cost $< w_Q$. This will either be the initial timestep where all voltage levels are kept and there is minimal SVC usage, or a case with no switching, low SVC usage and no voltage violations.
- **Low cost**, indicates a cost $> w_Q$, but $< w_{SVC}$. This indicates some reactive component switching and very little SVC usage.
- **Medium cost**, indicates a cost $> w_{SVC}$, but $< 10 \times w_{SVC}$. Medium cost indicates heavy reactive component switching or some SVC usage.
- **High cost**, indicates a cost $> 10 \times w_{SVC}$. High cost may indicate voltage breaches and/or heavy SVC usage.

For each model, an overview of how many times each cost level occurs will be included. This gives a good indication of the behavior of the controller, whether it handles the power changes without excessive switching and voltage violations.

Time

The time elapsed for each time series will be logged. Here a histogram is plotted to give an indication of how long each simulation series took (all timesteps, including the initial optimization).

Voltage level

As the very heart of the control problem is to keep the voltage level within its bounds, the voltage level is plotted. The voltage levels are displayed in a histogram and indicate the number of times the voltage at one bus is that very voltage level. Bus number 16 is left out of the plots, as this is the slack bus, and the voltage level is set to $1pu = 410kV$.

A plot indicating the average voltage level of each optimization is also included.

Reactive power

The reactive power generated and consumed by the on/off components will be displayed. This gives an overview of how frequent the components are active. An overview of the highest number of capacitors and reactors will also be presented. This will show if the controller saturates.

Switching and SVC usage

The average number of switchings in each series will be plotted in a histogram. Switching in the initial timestep will be excluded, as this does not lead to an increasing cost. For the models containing SVCs the total SVC usage will be plotted as well.

Real Power loss

The sum of real power throughout the network will be plotted to give an overview of the average loss in the system, even though a direct comparison to general power system losses will be difficult, due to different networks and lack of autotransformers etc.

Key values

A table containing key values that evaluates the performance of the controller is included. Here, the rate and number of voltage violations, maximum reactive component use and possible competing components are displayed.

7.2 Centralized voltage control

The first controller presented will be the centralized controller based on the full system model.

7.2.1 System model with SVCs

The first case will handle the control problem including the SVCs. The power demands are the same in both cases, and the statistics included will be of the same variables, except the SVC reactive power utilized.

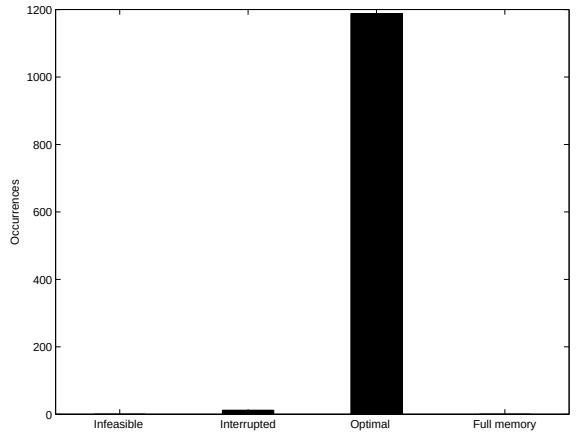

Figure 7.1: Status for all timesteps in the simulations - Centralized model with SVCs

As seen in figure 7.1, all the optimization were able to produce a solution. Most of the solutions converged to the best possible value within the given timeframe.

All of the optimal solutions were found with little or no cost (figure 7.2). Since voltage violations were minimal, these played a small part in the total cost of the objective.

Most simulations (all timesteps including the initial optimization) finished within 15 minutes, as displayed in figure 7.3.

As the main objective for the optimal controller is to maintain the voltage level, figures 7.4 and 7.5 shows that the voltage levels stay within their boundaries. Figure 7.5 shows that the average voltage levels lie generally in the middle of the operating area. However, figure 7.4 shows that sev-

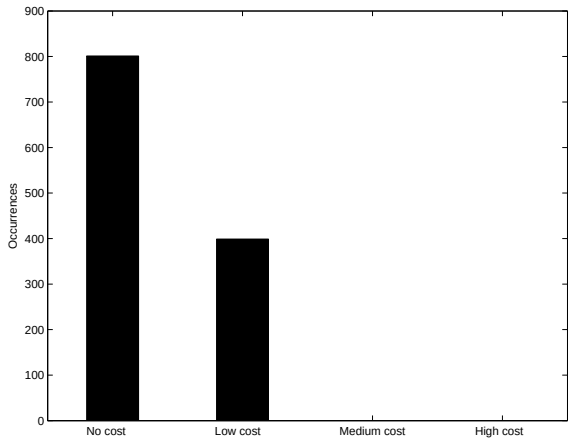

Figure 7.2: Cost of every timestep - Centralized model with SVCs

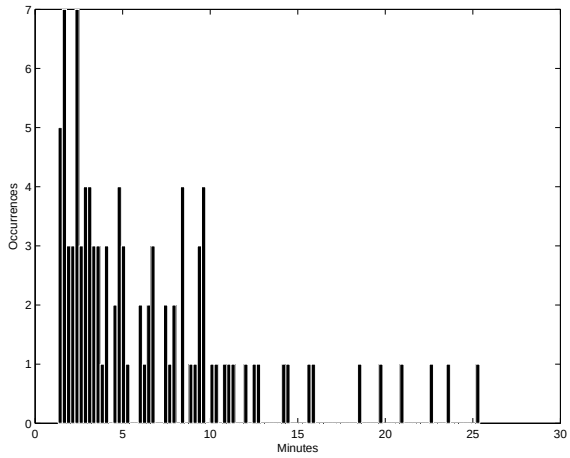

Figure 7.3: Time elapsed for every simulation - Centralized model with SVCs

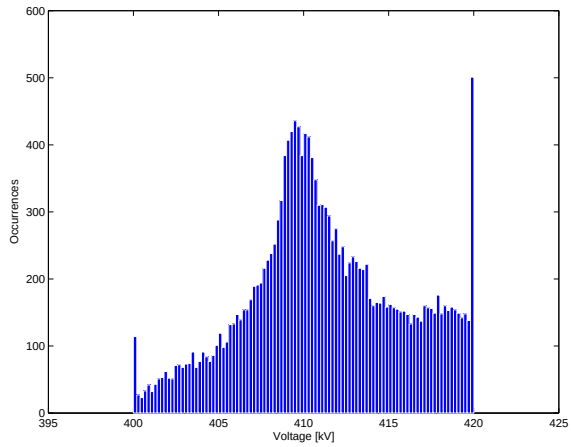

Figure 7.4: Voltage level in every bus, every timestep (except the slack bus) - Centralized model with SVCs

eral occurrences lies on the voltage boundaries. This can be explained by the SVC usage, which uses as little reactive power as possible to keep the voltages just within their nominal values.

The capacitor usage in the system is generally high, as seen in figure 7.6. An average per simulation uses up to 20 connected components. The use of reactors are very limited, and in most cases no reactors are used, see figure 7.7. Even though the total values of connected components are large, the bus with the most components (usually bus 6) does not have more than 5 capacitor batteries coupled, as seen in figure 7.8.

In spite of high number of total capacitors in the network, average switchings made from one timestep to the next are kept at relatively low values, seldom more than one. This indicates that the controller actions needed to maintain the voltage levels are limited. Reactive component switching is presented in figure 7.10.

From figures 7.11 and 7.12 it can be seen that the total SVC usage is kept at an almost imperceptible amount. Even so, the little reactive power

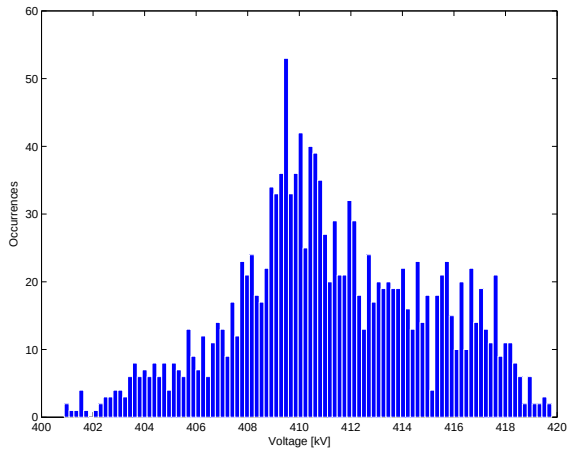

Figure 7.5: Average voltage level in the system, every simulation (except the slack bus) - Centralized model with SVCs

applied keeps the voltage level below the boundaries. Table 7.1 shows that the number of voltage violations are close to zero.

The average real power loss is also plotted, see figure 7.13. However, due to the different characteristics of the network model (less lines and buses), the power loss are difficult to compare to the loss in the actual Southern Norwegian power grid.

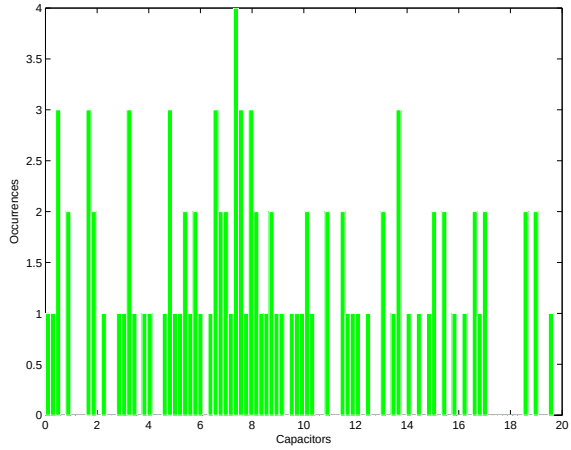

Figure 7.6: Average number of capacitors coupled in the system, every simulation - Centralized model with SVCs

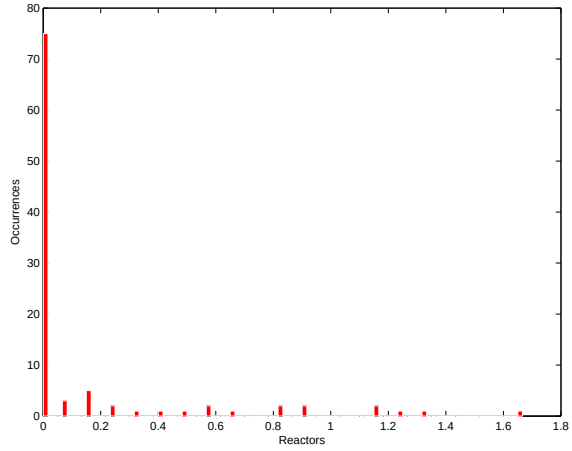

Figure 7.7: Average number of reactors coupled in the system, every simulation - Centralized model with SVCs

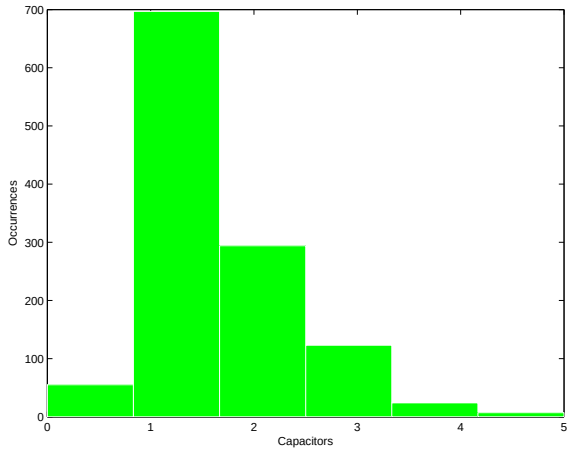

Figure 7.8: Largest number of capacitors in one bus, every timestep - Centralized model with SVCs

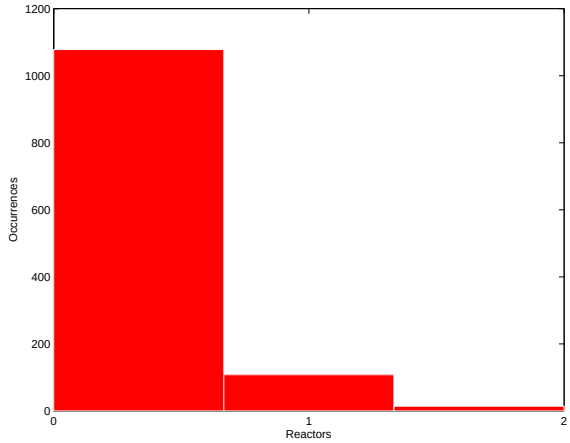

Figure 7.9: Largest number of reactors in one bus, every timestep - Centralized model with SVCs

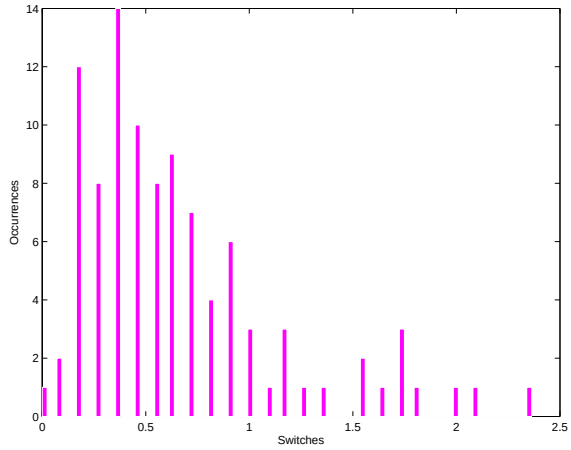

Figure 7.10: Average number of switchings performed (not including the initial timestep), every simulation - Centralized model with SVCs

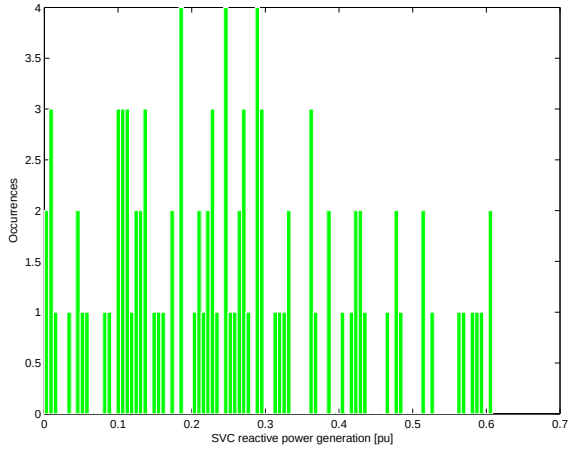

Figure 7.11: Average SVC reactive power generation, every simulation - Centralized model with SVCs

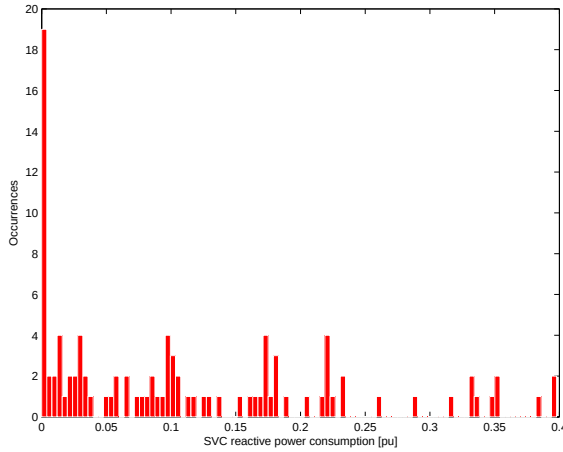

Figure 7.12: Average SVC reactive power consumption, every simulation - Centralized model with SVCs

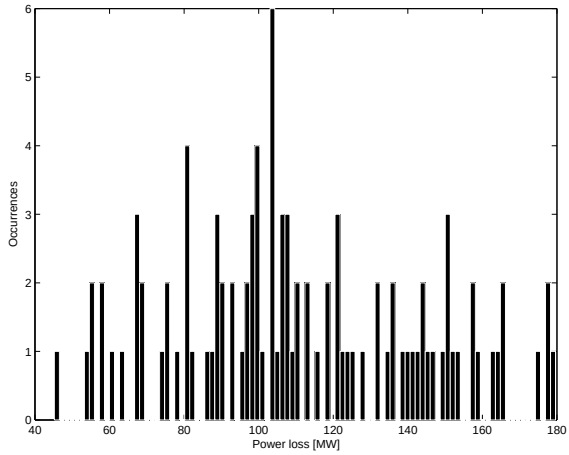

Figure 7.13: Average real power loss, every simulation - Centralized model with SVCs

Description	Numeric Value
Voltage violations, one bus - one optimization/timestep ($> 0.1kV$)	0
Voltage violations, one bus - one optimization/timestep ($> 0.05kV$)	0
Voltage violations, one bus - one optimization/timestep ($> 0.01kV$)	0
Highest number of capacitors in one bus	5
Highest number of reactors in one bus	2
Total number of optimizations	1200
Total number of voltage levels controlled	19200
Number of cases where both reactors and capacitors are coupled	97
Rate cases where both reactors and capacitors are coupled	$\frac{97}{1200} = 8.08\%$
Rate of voltage violations ($> 0.01kV$)	$\frac{0}{19200} = 0\%$

Table 7.1: Table of key numbers - Centralized model with SVCs

7.2.2 System model without SVCs

In this section the system model is run with the same power demands on the model without the SVCs.

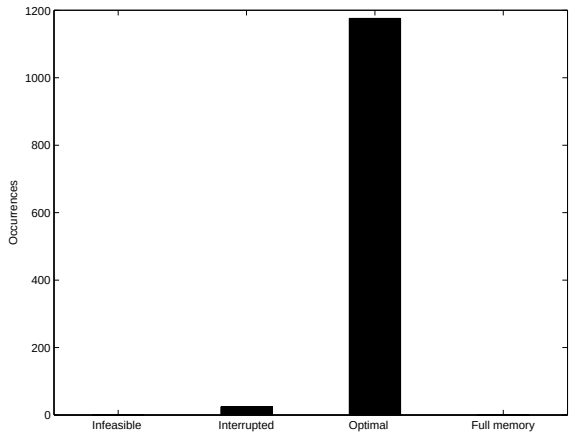

Figure 7.14: Status for all timesteps in the simulations - Centralized model without SVCs

When excluding the continuous decision variables from the optimization, the number of optimizations not converging within the time limit increases slightly (12 to 24 incidents). So does the average runtime for each simulation. In figures 7.14 and 7.16, the status and time spent is displayed, respectively. Even though the number of occurrences with "interrupted case" and the total time spent has increased, in comparison between the SVC model, the controller is able to produce sound outputs in close proximity to the "best possible" values.

From the cost overview of the simulations, in figure 7.15, it can be seen that the number of occurrences with "no cost" has decreased, in comparison with figure 7.2. This can be explained by the controller's inability to control minor voltage violation with minor SVC usage, and therefore needs to perform switches.

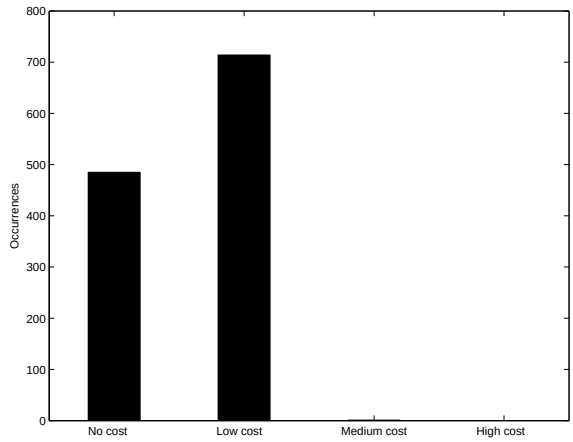

Figure 7.15: Cost of every timestep - Centralized model without SVCs

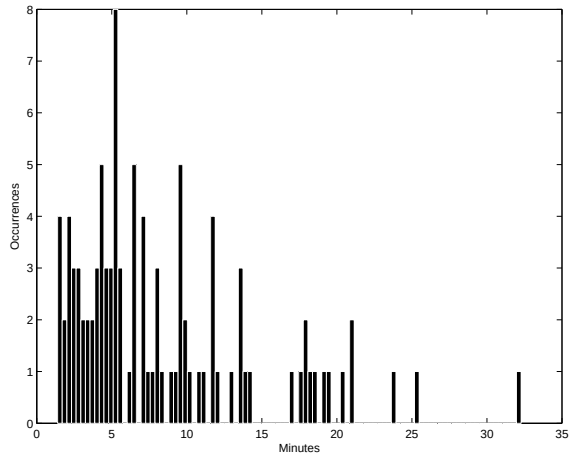

Figure 7.16: Time elapsed for every simulation - Centralized model without SVCs

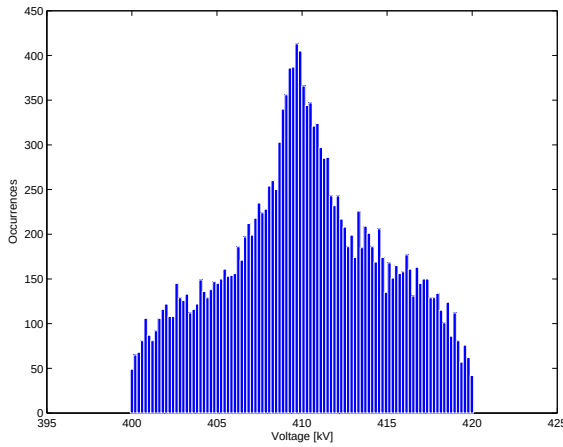

Figure 7.17: Voltage level in every bus, every timestep (except the slack bus) - Centralized model without SVCs

Even if both the average cost, and time spent has increased without the SVCs, the voltage levels avoid more boundary incidents using this scheme. This is explained by the same phenomenon as the cost function; minor voltage violation needs to be controlled by major control action, i.e. coupling a capacitor or reactor. This again means the controller cannot control the voltage level to the boundary, as is possible with a continuous control output.

Comparing the number of capacitors and reactors coupled, see figure 7.19 and 7.20, to the previous scheme, in figures 7.6 and 7.7, the values varies minimally. So does the maximum number used in each bus, figures 7.21 and 7.22. However, the number of switchings performed, in figures 7.23 (non-SVC case) and 7.10 (SVC case), it is generally a little higher for the model without SVCs.

The power loss in both models, figure 7.24 and 7.13, yields very similar values.

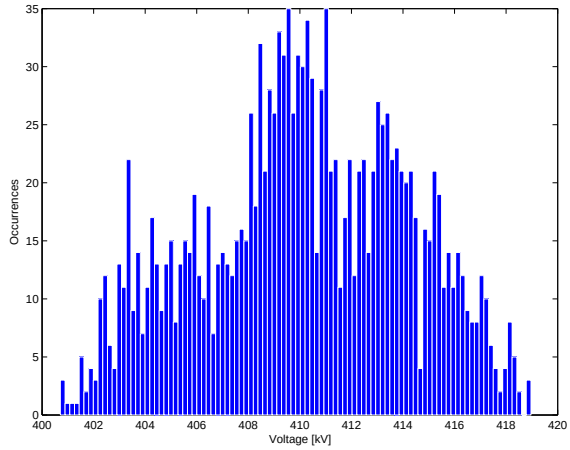

Figure 7.18: Average voltage level in the system, every simulation (except the slack bus) - Centralized model without SVCs

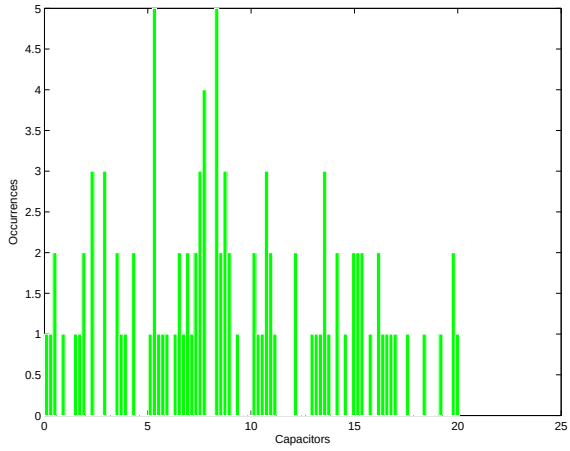

Figure 7.19: Average number of capacitors coupled in the system, every simulation - Centralized model without SVCs

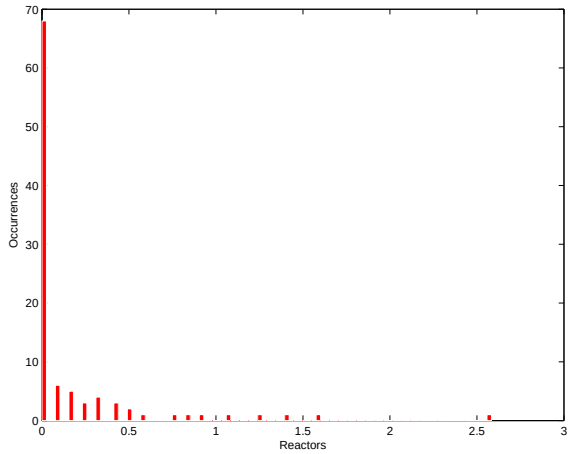

Figure 7.20: Average number of reactors coupled in the system, every simulation - Centralized model without SVCs

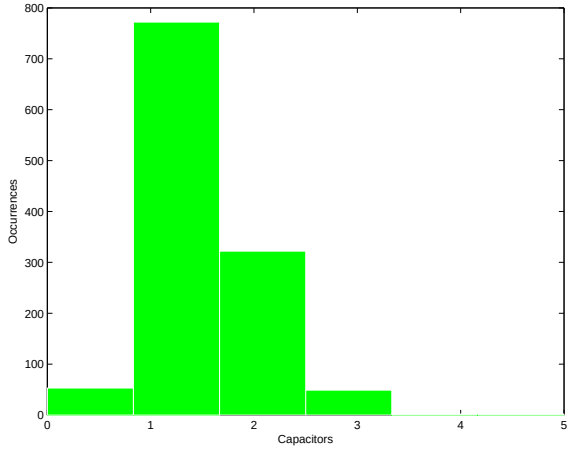

Figure 7.21: Largest number of capacitors in one bus, every timestep - Centralized model without SVCs

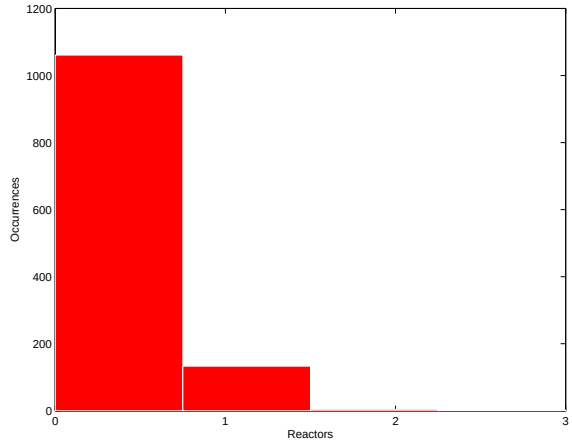

Figure 7.22: Largest number of reactors in one bus, every timestep - Centralized model without SVCs

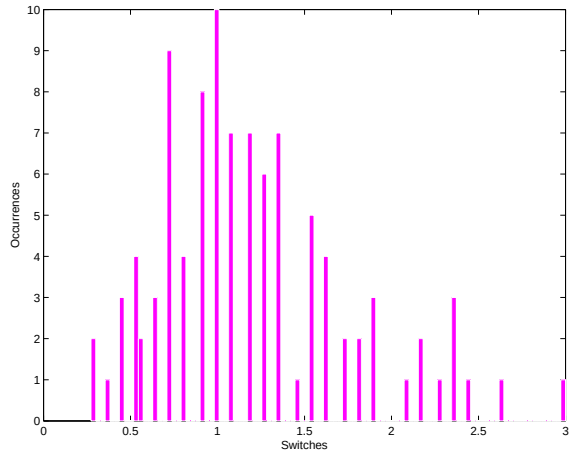

Figure 7.23: Average number of switchings performed (not including the initial timestep), every simulation - Centralized model without SVCs

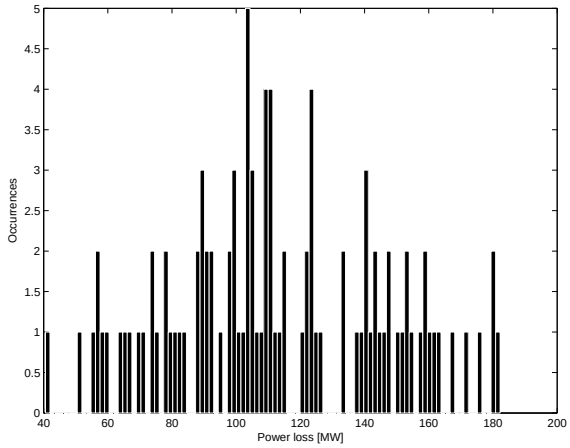

Figure 7.24: Average real power loss, every simulation - Centralized model without SVCs

Description	Numeric Value
Voltage violations, one bus - one optimization/timestep ($> 0.1kV$)	0
Voltage violations, one bus - one optimization/timestep ($> 0.05kV$)	7
Voltage violations, one bus - one optimization/timestep ($> 0.01kV$)	12
Highest number of capacitors in one bus	5
Highest number of reactors in one bus	3
Total number of optimizations	1200
Total number of voltage levels controlled	19200
Number of cases where both reactors and capacitors are coupled	104
Rate cases where both reactors and capacitors are coupled	$\frac{104}{1200} = 8.67\%$
Rate of voltage violations ($> 0.05kV$)	$\frac{7}{19200} = 0.03\%$
Rate of voltage violations ($> 0.01kV$)	$\frac{12}{19200} = 0.06\%$

Table 7.2: Table of key numbers - Centralized model without SVCs

7.3 Decentralized voltage control

The decentralized simulations will be run the same way as the centralized control scheme. The only alterations made to the system model are the available reactive components, see section 5.5. The power flows in the system will also be reduced in proportion to the centralized case, to better reflect a part of the Southern Norwegian power grid.

As well as making the argument that the decentralized voltage control case represents a controller in a small part of the power grid, it is also a good test as to how the controller operates with lighter loads and with limited supply of reactive components. As is previously mentioned, only the controller including SVCs will be tested.

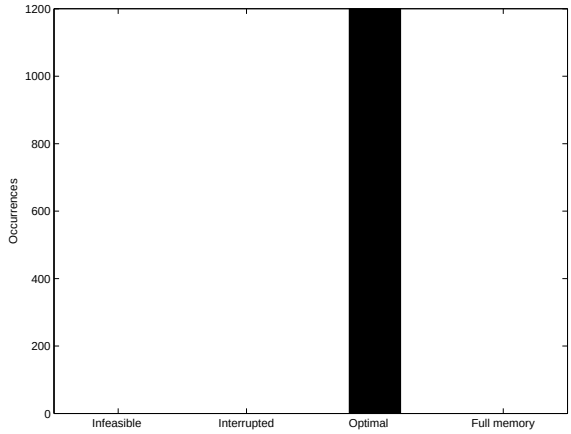

Figure 7.25: Status for all timesteps in the simulations - Decentralized model with SVCs

Optimal solutions were found for all optimizations, the cost was either low or close to zero. All simulations also finished within a 2 minutes time span. This is displayed in figures 7.25, 7.26 and 7.27, respectively.

All voltage levels were kept well within its bounds, and few voltage levels were on the limits, see figures 7.28 and 7.29.

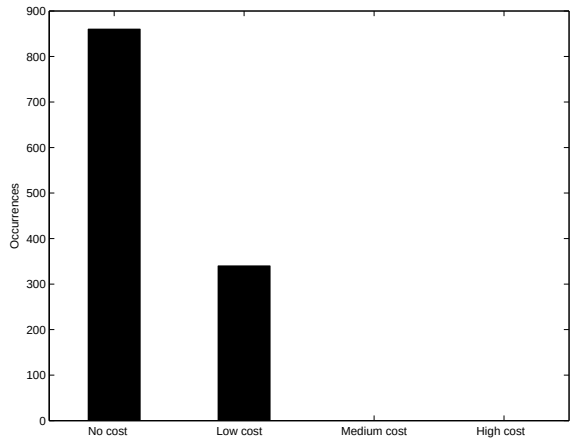

Figure 7.26: Cost of every timestep - Decentralized model with SVCs

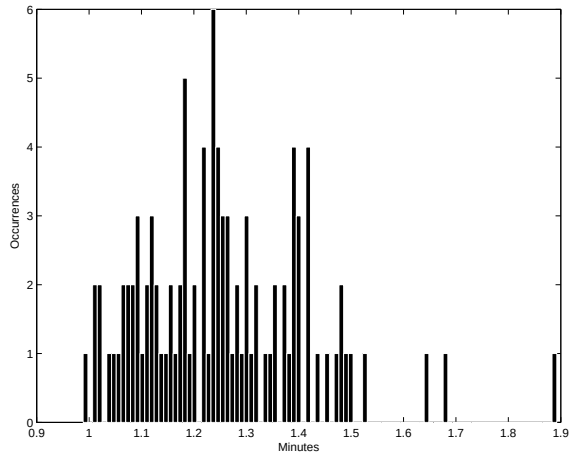

Figure 7.27: Time elapsed for every simulation - Decentralized model with SVCs

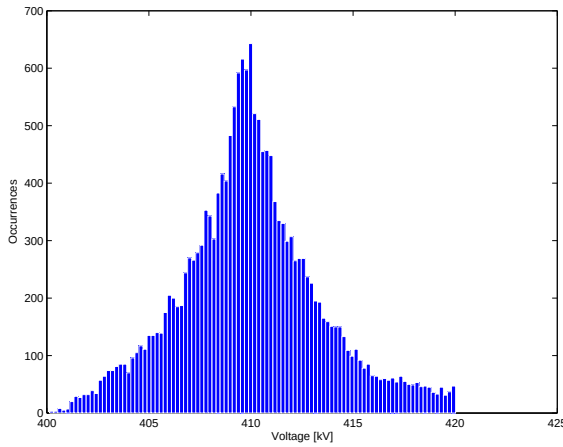

Figure 7.28: Voltage level in every bus, every timestep (except the slack bus) - Decentralized model with SVCs

Since these optimizations experienced lower load cases than the previous tests, the need for capacitors decreased, see figure 7.30. However, reactor usage (figure 7.31) was increased compared to the previous cases, see figures 7.7 and 7.20. In figure 7.32 and 7.33, it is seen that the largest number of capacitors and reactors used in one bus is 4 and 3, respectively.

Both switching and SVC usage is very limited in these simulations, as seen in figures 7.34, 7.35 and 7.36

Average real power losses in the system are plotted in figure 7.37.

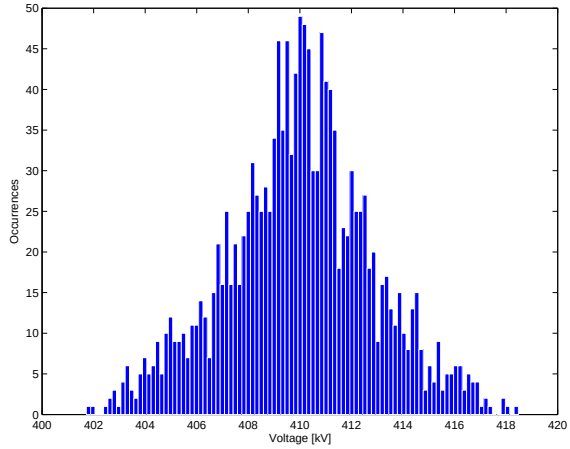

Figure 7.29: Average voltage level in the system, every simulation (except the slack bus) - Decentralized model with SVCs

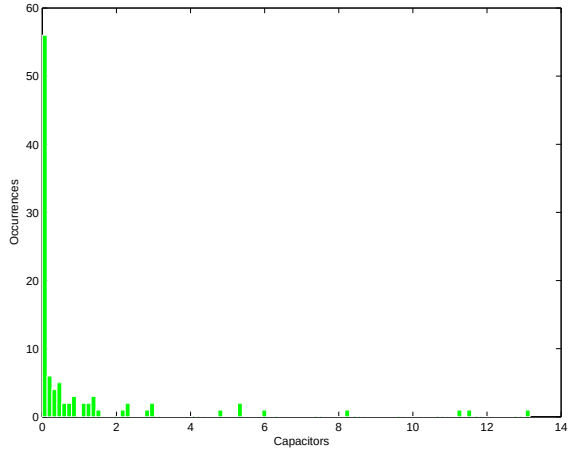

Figure 7.30: Average number of capacitors coupled in the system, every simulation - Decentralized model with SVCs

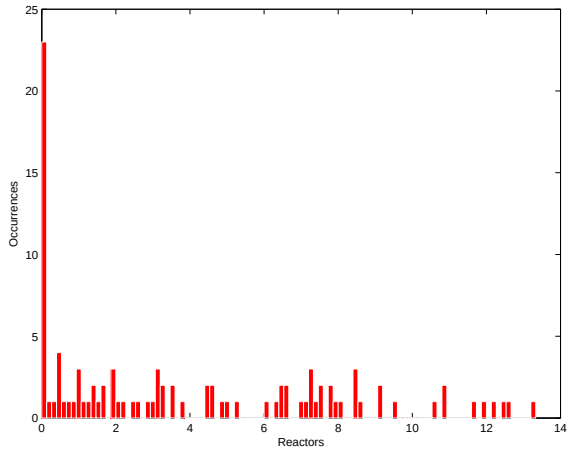

Figure 7.31: Average number of reactors coupled in the system, every simulation - Decentralized model with SVCs

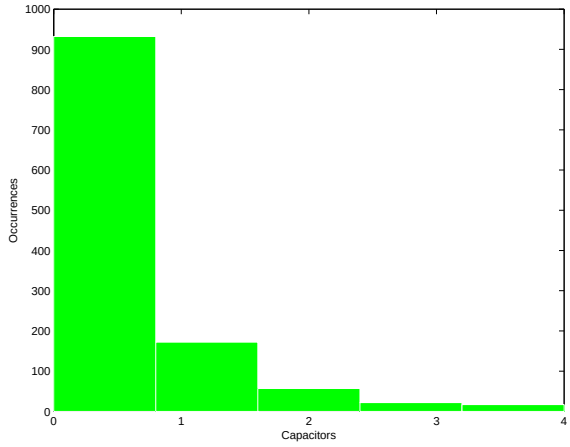

Figure 7.32: Largest number of capacitors in one bus, every timestep - Decentralized model with SVCs

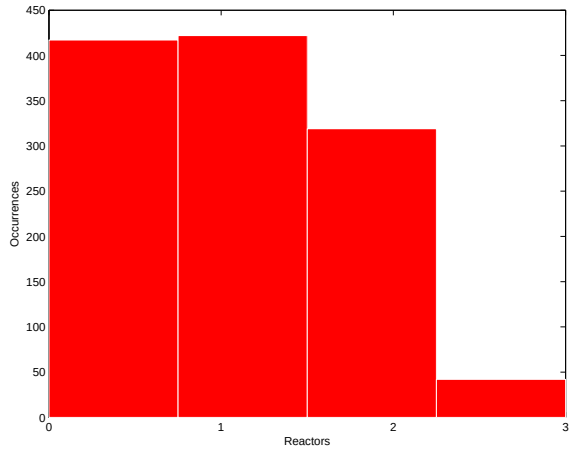

Figure 7.33: Largest number of reactors in one bus, every timestep - Decentralized model with SVCs

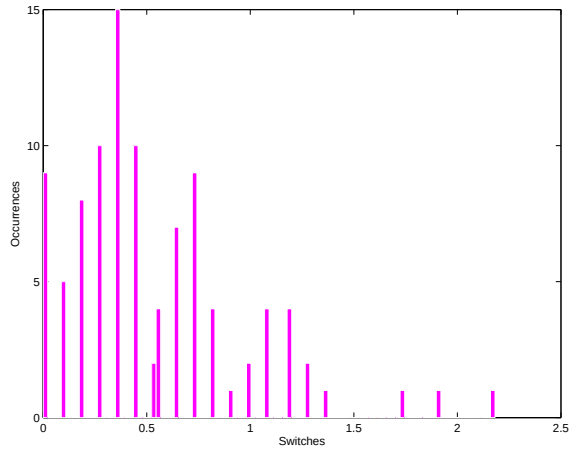

Figure 7.34: Average number of switchings performed (not including the initial timestep), every simulation - Decentralized model with SVCs

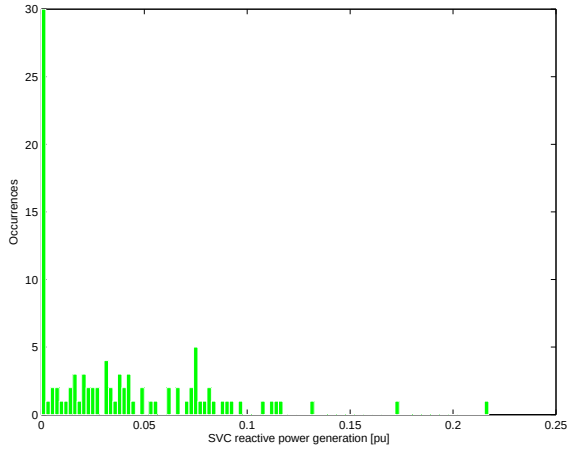

Figure 7.35: Average SVC reactive power generation, every simulation - Decentralized model with SVCs

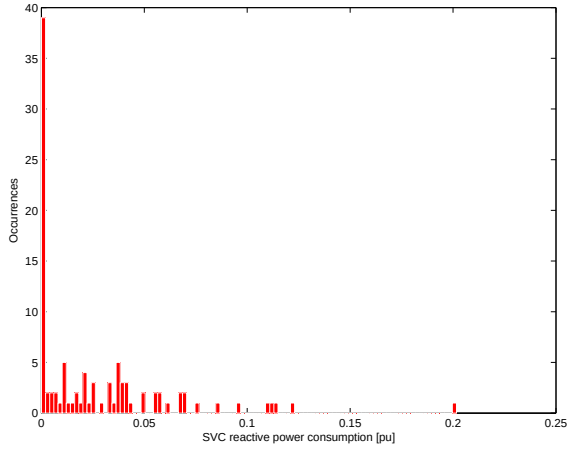

Figure 7.36: Average SVC reactive power consumption, every simulation - Decentralized model with SVCs

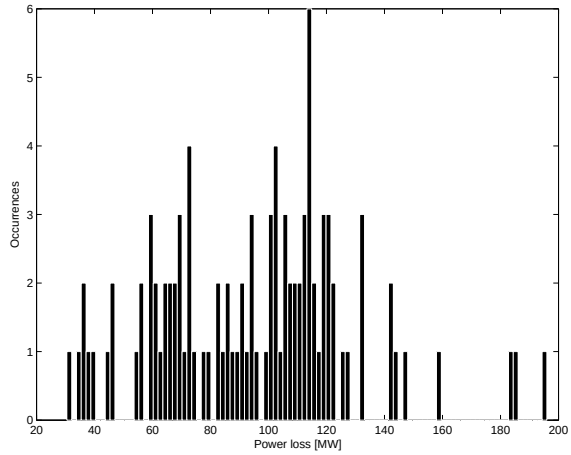

Figure 7.37: Average real power loss, every simulation - Decentralized model with SVCs

Description	Numeric Value
Voltage violations, one bus - one optimization/timestep ($> 0.1kV$)	0
Voltage violations, one bus - one optimization/timestep ($> 0.05kV$)	0
Voltage violations, one bus - one optimization/timestep ($> 0.01kV$)	7
Highest number of capacitors in one bus	4
Highest number of reactors in one bus	3
Total number of optimizations	1200
Total number of voltage levels controlled	19200
Number of cases where both reactors and capacitors are coupled	54
Rate cases where both reactors and capacitors are coupled	$\frac{54}{1200} = 4.5\%$
Rate of voltage violations ($> 0.01kV$)	$\frac{7}{19200} = 0.036\%$

Table 7.3: Table of key numbers - decentralized model with SVCs

Chapter 8

Analysis

After having presented the results in chapters 6 and 7, the analysis of the simulations will be presented in this chapter.

8.1 Centralized optimization model

An analysis will be made both for the simulated test cases and the Monte Carlo simulations, as well as an evaluation of the overall performance of the controller.

8.1.1 Test cases

Light load case

Using the system data from the light load case, the controller has no problems keeping the voltage limits, and keeps the reactive component switching to a minimum. There are very little difference between the problem formulation including the SVCs and the one without.

What stands out in the light load test cases is the controller's limited reactor usage. Given the low load data used in the optimization, a control scheme based mainly on reactors were to be expected. However, due to the system model being made up of a very limited number of power lines,

as opposed to the full system, the load on each line are relatively large compared to the expected Ferranti-effects, and will therefore not experience the expected overvoltage. Still the voltage levels react as predicted by decreasing as the power demand increases.

Note that controller actions will not be taken unless the controller experience voltage limit violations, or calculates that violation will be made unless the controller takes action. Closer examination of figure 6.1 shows that most voltage levels approach the low limit toward the final timestep. This is considered unproblematic as long as the limits are not breached. This feature is a directly related to the problem formulation of the controller, see equation (4.1.1), i.e. a switch will not be made unless it helps avoid voltage violations or limits SVCs usage. This phenomenon will not occur this quickly in a actual power grid, as these variations are taken from a 11 hour time span.

Heavy load case

By evaluating the heavy load case there is a clear indication that the power flows are on the limit of being too large to be handled by the reactive components available in the system. As for the light case, the line loads are greater than they would be on a network that includes more lines and buses. Even if this study evaluates an unrealistic scenario, the controller handles the voltage changes and is able to stay close to the given boundaries (when provided with enough control variables).

When introducing the SVCs, the controller is able to keep the voltage levels within its bounds, mainly because it has increased reactive power available for voltage control. It is also clear from the voltage levels in figures 6.14 and 6.20, that one bus especially experiences low voltage values. Closer examination indicates that this is bus number 6, i.e. the bus with the most - and longest connected power lines. These effects lower the voltage at a given bus when the power flows are large. At this bus, all capacitors available were used in timesteps 5-11, i.e. the controller saturated.

An interesting notion to this is that close to all other voltage levels lie close to its upper bound, despite it being a heavy load on the lines, this is

due to heavy capacitor coupling to keep the voltage level of bus number 6 over the lower limit. For the generator buses, the lack of AVRs (automatic voltage regulator, see section 2.2.3) will also lead to higher voltages when the production is high, as in this test case. An exception to this is bus 16, which is the $V - \delta$ slack bus and can be considered to have an AVR, as it is given a constant voltage of $410\,kV$.

Even though the number of capacitors used far exceeds the number of capacitors in the actual power grid, evaluating each bus shows that the reactive power compensation in the buses are only excessively large at buses with excessively large power demands, see appendix section A.4.

Computational time spent on the heavy case study also well exceeds the light case, and the SVCs model is much faster than the one with only integer reactive components. As the changes from one timestep to the next are far greater in the heavy case study, the new solution lies further from the previous and are therefore more difficult to obtain for the solver.

Another important note from the heavy case study is that the optimizing controller rather lets several voltage levels get slightly breached than let one get a large violation (see timestep 10 in figure 6.14). This comes as a characteristic of the quadratic cost function explained in section 4.2.1.

8.1.2 Monte Carlo

By running several Monte Carlo simulations, the goal is to try to unveil flaws in the system model or controller. The control scheme clearly experience more voltage drops than increases, which is indicated by more capacitors coupled than reactors. This is closely related to the power transmitted in the system, which is high due to the phenomenons explained in section 8.1.1. Even so, the main task of this thesis is to evaluate the use of an MINLP controller for the voltage control problem. Simulations indicate that the controller is able to produce reasonable inputs, and limit both the voltage violations and switching, in spite of extreme conditions.

Looking at the voltage levels for all buses in all the simulations with SVC, see figure 7.4, there are a large number of occurrences on both the lower and upper voltage limit. A closer examination of the results tells us,

not surprisingly, with an eye on the test cases in section 8.1.1, that bus number 6 lies at the lower limits at a great amount of the time.

SVC usage in the controller that included SVCs was almost neglectable. Since the reactive on/off components were far from saturated, this is the desired result and means SVCs are available if needed, see section 2.2.2. Even so, the usage is great enough to provide boundary condition in the voltage levels, see section 7.2.1.

The occurrences of optimizations with both reactors and capacitors are displayed in tables 7.1 and 7.1. These show that $\approx 8\%$ of all optimizations have both reactors and capacitors coupled. This is a high number compared to desired respons of a system wide voltage controller. However, due to lack of AVRs and the fact that some buses will experience "summer conditions" (light loads) while other experience "winter conditions" (heavy loads) will cause different voltage compensation demands throughout the power grid.

Another important notion is that the controller does not saturate in any of the Monte Carlo test cases, as it did in the heavy load test case, see section 8.1.1. This means the supposedly excessive number of capacitors, in section 5.3, might not have been justifiable, but was necessary to control the heavy test case. The largest number of capacitors coupled in one bus was 5, this occurred a very limited amount of times, see figures 7.8 and 7.21.

All the optimizations terminated due to excess computational time were in close proximity to the "best possible" solution, i.e. the controller was able to produce sound output, despite failing to converge within the given time.

8.2 Decentralized optimization model

Utilizing the controller as a distributed model is an idea worth exploring. As previously mentioned this is not an unexplored area and can give great advantages in terms of computational time and system overview.

As the idea is to limit the loads on the lines, as well as limiting the availability of the reactive components, this simulation scenario are in many ways a continuation of the control system implemented for the full scale

model. Many of the actual system buses do not have reactive components for voltage control. As previously mentioned, it also lets the system handle lower power generation and demands.

With all this in mind, the Monte Carlo simulations used on the decentralized model might be the most realistic compared to the actual power grid. It provides limited access to reactive components, realistic line loads and reasonable spread of reactor and capacitor usage.

The MINLP controller gave very satisfactory results for this control scheme. Despite sparse reactive component availability, the voltage levels were kept within the limits, and the reactive switching was kept at a minimum.

In these simulations the controller also shows its ability to use both inductors and capacitors for voltage control. Still, closer examination of the simulation numerics shows that few instances need use of both reactors and capacitors, which is the desired result.

From this case it was clear that reducing the number of decision variables reduces the computational time. Comparing this controller to the centralized model with SVCs (that has the twice the number of integer decision variables) it is seen that the simulation time for 11 timesteps plus the initial optimization, are reduced from an average of 5-10 minutes to well 1 minute, see figures 7.3 and 7.27.

Chapter 9

Discussion

In this chapter a evaluation and comparison of the numerical results and the analysis in chapters 6- 8, is presented. A discussion of the use of an MINLP controller as opposed to other options will also be discussed. Also some notes on applicational considerations for the MINLP controller, both for implementation and operation, are included.

9.1 Centralized MINLP controller

The two predetermined case studies gave the MINLP controller possibilities to operate at reasonable operating conditions in the light case, and unreasonable operating conditions in the heavy case. Nevertheless, the optimal controller handled both cases by keeping the voltage limits, and not making excessive couplings. The SVC usage was also kept at a minimum, which indicates that the MINLP controller can operate by basing the controller actions solely on capacitors and reactors.

In the Monte Carlo cases the power transmitted, and the power changes from one timestep to the next, is extreme. The controller is still able to keep the bounds, and does so generally with reasonable reactive power usage. As the physics of the system indicates, the reactive power compensation needed at each bus, is in proportion to the real power transmitted.

As expected, voltage increases of the same magnitude as the voltage drops does not occur. This is because the capacitive loads at each end of the π-equivalent, see section 4.3.1, can be compensated by a given inductive load. However, the inductive effect on the power lines knows no boundaries as they grow with the loads on the lines.

A side note is that as the system model has two real power slack buses, these will generate real power according to the best possible voltage levels throughout the network. This is not directly related to practice of voltage control, but does not cause unrealistic scenarios throughout the simulations and is not regarded as a decisive factor for the voltage levels throughout the power system.

As a proof of concept, the MINLP controller gives satisfactory results for both the test cases and the Monte Carlo simulations. This indicates that the controller can function by taking only integer decisions, and can include support for SVC limitation. With the number of decision variables in the actual power grid being of the same order of magnitude, the computational time should not increase significantly. Therefore the use MINLP for solving online power flow problems with regards to voltage control seems to be a feasible task, even in a full scale power grid.

9.2 Comparison to other control schemes

9.2.1 Automatic, non-optimal controller

Implementing an optimal controller as opposed to an automated switcher, could lead to great economic and environmental benefits. The automated switcher has provided reasonable voltage control, keeping the voltage levels within the limits. By using an optimal controller, the number of control actions taken can be reduced, leading to less downtime and lower maintenance costs. The optimal controller will always use the least possible number of components that keeps the voltage levels. This, combined with it reducing SVC usage, means the power grid maintain its maximum potential for additional voltage alterations.

9.2.2 Distributed controller

Advantages of the distributed controller

The decentralized model would, from an operator's point of view, give a better understanding as to which reactive components control which bus voltages. Also, the overview of where the system limitations are, in terms of reactive compensation, would be easier to follow, as the scheme work more similar to the current - manual control. Computational time would decrease, as different solvers solve small optimization problems instead of one controller solving one large. A decentralized controller also removes the "single point of failure" problematics imposed by a centralized controller [20]. This means if one controller goes down, the rest of the system is still operative.

Disadvantages of the distributed controller

As the whole system network is a coupled system, voltage variations will occur throughout the system when reactive couplings are made. Utilizing a decentralized controller, could lead to incidents where there are available reactive components in one bus, which can help control the voltages in the next. If these buses are regarded as in different zones, the connection will not be made to control the voltage level as the controller at this zone does not know of the available reactive component. Despite the distributed schemes advantages is terms of removing "single point of failure" problematics, each controller require maintenance and updates. A centralized controller would therefore only be one entity to keep up to date.

9.3 Applicational considerations

When applying the optimal voltage controller to the actual power grid there are some considerations to be taken care of.

First of all one has to decide whether the controller should be used as user support for the operator or as an automatic controller. Though the controller was made with automation in mind, an optimal controller would

also provide a good connection scheme for the operator, limiting his or her control actions and reducing the wear and tear of the components.

Utilizing this controller on the physical network, the controller actions will be taken after the power demands are measured, and voltage levels have already dropped. To avoid the few seconds to minutes of violation this could lead to, it is possible to move the controller voltage limits within the nominal area. This would mean the controller takes action when the voltage levels approach the limits, not when they are breached.

If deciding to use a decentralized controller, the next step should be to investigate the decoupling of the power grid, i.e. where are the power lines that cause the least amount of voltage variations between the connected buses.

Using the optimization with its current problem formulation would distribute the controller actions between several buses, see section 4.2.2. This could lead to greater periods of time where only one component is the bus is switched in and out of the system. This would again lead to great wear and tear of the component in question. By implementing a queuing system for the control components in each bus, the damage can be distributed on all components.

From an operator's point of view, a change from what was until recently, a manual controller to a completely automated and optimal environment would be a big step. Ensuring that the operators trust - and have the proper tools to operate the controller is essential. Making it as user friendly as possible, by for example highlighting reactive couplings and displaying why these are made could be the difference from the operators wanting to implement an optimal controller, or wanting to stick to the status quo.

Chapter 10

Conclusion

This thesis shows that while MINLP is a challenging field, it has proven possible to solve voltage control problems of this size in satisfactory manner. Even though global optima cannot be proven found, the problem only requires heuristic solutions. Allowing this, as well as allowing termination on solution close to the best bound ensures reasonable runtime and satisfactory results.

Even though an exact comparison between the system model and the coupling scheme in the actual power grid is difficult to produce given the different models, simulations indicate that the optimal voltage controller is able to keep the voltage level within the given bounds, without making excessive couplings. The system model including the SVCs also shows promising results in limiting SVC usage.

Tuning the optimization algorithm would also optimize behavior of the controller. All the simulation schemes clearly indicate that keeping the voltage limits is the prioritized task. By finding the optimal relationship between the weights, slight breaches of the voltage limits could be allowed to keep the system from immediately switching the reactive component.

Given that a study of the decoupling in the Southern Norwegian power grid is performed, using a decentralized optimizer is also an interesting alternative. This will allow the solver to move close to its bound on an

even shorter timeframe.

MINLP solvers and algorithms will continue its development, and the computational power of the computers running these will increase. As mentioned in the introduction, the voltage control problem continues to grow and the work load on the operators increases. All in all, this thesis provides a solid proof of concept in using a challenging field, under rapid development, as a solution to a problem due for a change in solution method.

Chapter 11

Further work

As only a proof of concept for the MINLP controller is provided in this thesis, there are some additional challenges that still needs to be addressed before implementing the controller on a physical grid.

11.1 Testing a full scale network

By investigating the controller at a full scale network model, a further - and more thorough evaluation of the algorithm runtime can be provided. Adding the additional system buses may decrease the controller's ability to provide feasible solutions at an acceptable runtime. Even so, as the number of integer decision does not increase significantly, the runtime should stay in the same order of magnitude.

By testing the full scale network, the real control components at each bus can be included to give a better approximation to the Norwegian power grid. This proved difficult in a limited network, as used in this thesis.

11.2 Future expansions

There are also some elements about the actual controller algorithm that can be further explored. Some of these will quickly be presented in this

section.

11.2.1 Smoother voltage levels

In spite of keeping the voltage limits and providing good controller outputs, the test cases shows fluctuations in voltage levels. Smoother voltage levels can be provided by changing the voltage bounds, or imposing an additional small cost for violations from $1pu$, or $410kV$. For example, by changing the part of the objective functions that penalizes voltage violations (see equation (4.1.1)) to the following:

$$w_V \sum_i \epsilon(i)^2 \quad \Rightarrow \quad w_V \sum_i \epsilon(i)^2 + w_{Vs} \sum_i (1pu - V(i))^2 \tag{11.2.1}$$

Where w_{Vs} is a small weight, but large enough to allow moderate reactive switching. This would allow the controller to take action even if voltage limits are not breached.

11.2.2 Time increasing voltage costs

A different approach to the cost function could be to increase the cost continuously over time as the voltage limits are breached. This would also reflect the way breaches of the voltage limits are measured by Statnett, in minutes away from nominal levels [37].

On the other hand, this would introduce more variables to log for the controller and increase the complexity as the demands for controller dynamics would increase.

11.2.3 Controllers

Developing a MPC (Model Predictive Controller [20]), or similar controller, would also be an interesting study, as the power demands over the course of 24 hours is somewhat predictable. However, utilizing this with an MINLP will require a lot of computational power. It is also a relatively unexplored field.

Appendix A

Numerical values and power system theory

A.1 Power flow equations

A.2 Per unit calculations

This chapter can be found in [14]. In electrical engineering, and power transmission, per unit calculations are often used to simplify the calculations [15]. By using base values instead of electrical quantities it is easy to include a larger network with units of different voltage levels. It also makes the numerical values of a power system easier to handle.

Typically, base values for the power and the voltage are selected as follows:

$$\begin{aligned} V_{base} &= 1pu \\ S_{base} &= 1pu \end{aligned} \tag{A.2.1}$$

The voltage base would often be the nominal value of a bus/node in a power system, for example $V_{base} = 420kV$ or $V_{base} = 300kV$. The base for power considerations will often be selected to reflect the power transmitted

in the power lines. Impedance, Z, and admittance, Y, are calculated as follows:

$$\begin{aligned} Z_{base} &= \frac{V_{base}^2}{S_{base}} = 1pu \\ Y_{base} &= \frac{1}{Z_{base}} = 1pu \end{aligned} \tag{A.2.2}$$

A.3 Line lengths

$$\begin{aligned} l_1 &= 35\ [km] & l_2 &= 88.5\ [km] \\ l_3 &= 12.5\ [km] & l_4 &= 36.5\ [km] \\ l_5 &= 11\ [km] & l_6 &= 107.5\ [km] \\ l_7 &= 42\ [km] & l_8 &= 66\ [km] \\ l_9 &= 98\ [km] & l_{10} &= 24.5\ [km] \\ l_{11} &= 93\ [km] & l_{12} &= 38.5\ [km] \\ l_{13} &= 31.5\ [km] & l_{14} &= 60\ [km] \\ l_{15} &= 46\ [km] & l_{16} &= 10\ [km] \\ l_{17} &= 24.5\ [km] & l_{18} &= 22\ [km] \\ l_{19} &= 27.5\ [km] \end{aligned} \tag{A.3.1}$$

A.4 Test case power demands

	Vest Agder	Aust Agder	Vestfold	Østfold	Oslo	Drammen	Oppland	Oppland North
timestep	1	2	3	4	5	6	7(G)	8
1	820	-40	-375	-330	-800	-470	660	-235
2	830	-40	-375	-375	-900	-500	660	-260
3	865	-40	-400	-430	-940	-550	670	-290
4	920	-40	-420	-500	-1000	-570	660	-320
5	950	-75	-500	-400	-950	-590	660	-340
6	970	-80	-450	-410	-975	-580	670	-340
7	990	-300	-475	-390	-1000	-600	690	-330
8	950	-400	-475	-380	-975	-610	700	-335
9	950	-200	-450	-360	-1050	-640	700	-340
10	950	200	-495	-375	-1050	-620	700	-330
11	950	200	-500	-390	-1100	-600	675	-330
12	950	0	-490	-400	-1075	-600	670	-330
	Hardanger	Sogn og Fjordane	Sogn og Fjordane	Bergen	Hordaland South	Rogaland North	Stavanger	Rogaland South
timestep	9(G)	10	11(G)	12	13	14(G)	15	16(G)
1	slack	-35	450	-1000	-200	1170	-1000	slack
2	slack	-50	450	-1000	-200	1380	-1000	slack
3	slack	-65	440	-1150	-200	1670	-1150	slack
4	slack	-65	475	-1200	-200	1840	-1200	slack
5	slack	-70	485	-1220	-200	2400	-1220	slack
6	slack	-70	495	-1200	-200	2270	-1200	slack
7	slack	-60	490	-1175	-200	2280	-1175	slack
8	slack	-45	465	-1200	-200	2200	-1200	slack
9	slack	-55	480	-1220	-200	2200	-1220	slack
10	slack	-55	480	-1200	-200	2180	-1200	slack
11	slack	-50	470	-1300	-200	2160	-1300	slack
12	slack	-50	475	-1350	-200	2170	-1350	slack

Table A.1: Power demands $[MW]$ - Light case study

	Vest Agder	Aust Agder	Vestfold	Østfold	Oslo	Drammen	Oppland	Oppland North
timestep	1	2	3	4	5	6	7(G)	8
1	-1462,5	1125	-1500	-750	-1875	-1050	675	-862,5
2	-1575	1350	-1875	-825	-2025	-1200	787,5	-937,5
3	-1725	825	-1875	-975	-2100	-1275	862,5	-1050
4	-1837,5	975	-1875	-1125	-2250	-1350	900	-1050
5	-1837,5	600	-1875	-900	-2250	-1350	900	-1050
6	-1837,5	225	-1875	-975	-2250	-1350	937,5	-1050
7	-1837,5	-150	-1875	-862,5	-2250	-1350	937,5	-1050
8	-1762,5	0	-1875	-862,5	-2250	-1350	937,5	-1050
9	-1800	-75	-1875	-862,5	-2250	-1350	937,5	-1050
10	-1837,5	112,5	-1875	-862,5	-2250	-1350	1012,5	-1162,5
11	-1912,5	-75	-1875	-862,5	-2400	-1350	1087,5	-1200
12	-1912,5	375	-2025	-862,5	-2325	-1350	1087,5	-1200

	Hardanger	Sogn og Fjordane	Sogn og Fjordane	Bergen	Hordaland South	Rogaland North	Stavanger	Rogaland South
timestep	9(G)	10	11(G)	12	13	14(G)	15	16(G)
1	slack	-75	450	-1125	-225	3000	-1125	slack
2	slack	-75	675	-1125	-232,5	3375	-1125	slack
3	slack	-93,75	975	-1275	-240	4125	-1275	slack
4	slack	-112,5	1050	-1350	-225	3750	-1350	slack
5	slack	-112,5	1125	-1350	-236,25	3937,5	-1350	slack
6	slack	-112,5	1350	-1350	-240	4125	-1350	slack
7	slack	-150	1425	-1350	-232,5	4125	-1350	slack
8	slack	-150	1425	-1350	-217,5	4050	-1350	slack
9	slack	-150	1425	-1350	-225	4050	-1350	slack
10	slack	-150	1350	-1350	-232,5	4200	-1350	slack
11	slack	-150	1350	-1500	-240	4125	-1500	slack
12	slack	-150	1500	-1500	-225	4350	-1500	slack

Table A.2: Power demands $[MW]$ - Heavy case study

Appendix B

Scripts

B.1 AMPL

```
1     # An Ampl version of Automatic voltage control
2         # Get askparm1.dat file for parameter settings
3
4   reset;
5
6
7   param G {i in 1..16, j in 1..16}; # Conductance
8   param B {i in 1..16, j in 1..16}; # Suceptance
9
10  param time; # current time
11  param totaltime; # Total timesteps
12
13
14  param run; # current run
15
16  param case; # current case called from bash command
17
18  param Qcap {i in 1..16}; #pi equivalent cap
19
20  param Qprev {i in 1..16};
21  param Vref {i in 1..16}; # Nominal Voltage
22
23  param LQ; # Limits for number of Reactors
```

```
24      param UQ; # Limits for number of capacitor banks
25      param Lsvc; # Limits SVC
26      param Usvc; # Limits SVC
27      param save; #ensures smooth objective function
28
29      param Vmin; # Nominal Voltage min
30      param Vmax; # Nominal Voltage max
31
32
33      param Pdem {i in 1..16,j in 1..totaltime}; # Real power demand
34
35
36
37      param wV; # Weight voltage
38      param wQ; # Switching weight
39      param wsvc; # Weight for svc use
40
41
42
43      var P{1..16,1..totaltime};
44      var Q{1..16} integer >= LQ, <= UQ;
45      var Qsvc{1..16} >=Lsvc, <= Usvc;
46      var V{1..16} >=0;
47      var delta{1..16} >=-3.14, <=3.14;
48      var e{1..16};
49      var d{1..16};
50      var Qswitch{1..16};
51      var pos{1..16} binary;
52      var neg{1..16} binary;
53
54       minimize cost:
55          wV * (sum{i in 1..16}(e[i]^2)) + wsvc * sum{i in 1..16}((0-Qsvc[i])^2)
56          + 0.001 * (sum{i in 1..16}(Q[i]^2));
57
58
59
60      subject to
61
62       # Voltage error
63       voltageErrorMin{i in 1..16}: -e[i]+Vmin <=V[i];
64       voltageErrorMax{i in 1..16}: e[i]+Vmax >=V[i];
```

```
65
66
67      # Q Switching
68      Qcalc{i in 1..16}: Qswitch[i]=Qprev[i] - Q[i];
69
70
71
72      # Power demands
73      c1{i in 1..totaltime}: P[1,i]=Pdem[1,i]; # 9 and 16 are the surplus nodes
74      c2{i in 1..totaltime}: P[2,i]=Pdem[2,i];
75      c3{i in 1..totaltime}: P[3,i]=Pdem[3,i];
76      c4{i in 1..totaltime}: P[4,i]=Pdem[4,i];
77      c5{i in 1..totaltime}: P[5,i]=Pdem[5,i];
78      c6{i in 1..totaltime}: P[6,i]=Pdem[6,i];
79      c7{i in 1..totaltime}: P[7,i]=Pdem[7,i];
80      c8{i in 1..totaltime}: P[8,i]=Pdem[8,i];
81      c10{i in 1..totaltime}: P[10,i]=Pdem[10,i];
82      c11{i in 1..totaltime}: P[11,i]=Pdem[11,i];
83      c12{i in 1..totaltime}: P[12,i]=Pdem[12,i];
84      c13{i in 1..totaltime}: P[13,i]=Pdem[13,i];
85      c14{i in 1..totaltime}: P[14,i]=Pdem[14,i];
86      c15{i in 1..totaltime}: P[15,i]=Pdem[15,i];
87
88
89
90      #init power flow
91      cV: V[16]=1;
92      cdelta: delta[16]=0;
93      c9{i in 1..totaltime}: P[9,i] >= 0;
94      c16{i in 1..totaltime}: P[16,i] >= 0;
95
96      realpower{i in 1..16}: P[i,time]=sum{k in 1..16}
97       (V[i]*V[k]*(G[i,k]*cos(delta[i]-delta[k])
98       + B[i,k]*sin(delta[i]-delta[k])));         #real power flow
99
100     reactivepower{i in 1..16}: (Q[i]+Qcap[i]+Qsvc[i])=sum{k in 1..16}
101      (V[i]*V[k]*(G[i,k]*sin(delta[i]-delta[k])
102      - B[i,k]*cos(delta[i]-delta[k])));        # reactive power flow equations
103
104
105     data ("setcase.dat");
```

```
106         data ("param_new/askparam"& case &".dat");
107
108     option solver bonmin; # Choose BONMIN as the solver (assuming that
109                           # bonmin is in your PATH
110
111
112     #options set both ipopt-options and bonmin-option,
113     #for bonmin-options use bonmin. as a prefix
114     options bonmin_options "bonmin.allowable_gap 0.00099
115     bonmin.time_limit 900 bonmin.nlp_log_level 0 bonmin.num_resolve_at_root 10
116     max_iter=100";
117
118
119     option log_file ("logg_cont_new/run"&run&"/asklog"&run&time&".log");
120
121     option presolve 0;
122
123
124     solve;                # Solve the model
125
126     print cost > ("logg_cont_new/run"&run&"/cost"&run&time&".log");
127     print{i in 1..16} V[i] > ("logg_cont_new/run"
128                       &run&"/voltage"&run&time&".log");
129     print{i in 1..16} delta[i] > ("logg_cont_new/run"
130                       &run&"/delta"&run&time&".log");
131     print{i in 1..16} P[i,1] > ("logg_cont_new/run"
132                      &run&"/power"&run&time&".log");
133     print{i in 1..16} Q[i] > ("logg_cont_new/run"
134                   &run&"/reactive"&run&time&".log");
135     print{i in 1..16} Qprev[i] > ("logg_cont_new/run"
136                         &run&"/prev"&run&time&".log");
137     print{i in 1..16} Qswitch[i] > ("logg_cont_new/run"
138                         &run&"/switch"&run&time&".log");
139     print{i in 1..16} Qsvc[i] > ("logg_cont_new/run"
140                              &run&"/svc"&run&time&".log");
141     print _total_solve_elapsed_time > ("logg_cont_new/run"
142                           &run&"/time"&run&time&".log");
143
144
145     display case;
146     display time;
```

```
147
148
149
150     # Rerun the problem for multiple time instances
151
152
153     delete minimize cost;  #use for including cost of switching
154     redeclare minimize cost: wV * (sum{i in 1..16}(e[i]^2))
155     + wQ * sum{i in 1..16}(Qswitch[i]^2) + wsvc * sum{i in 1..16}((0-Qsvc[i])^2)
156     + 0.001 * (sum{i in 1..16}(Q[i]^2));
157
158     for {n in 2..totaltime}        {
159
160     #Setting power demands for new hour
161
162        drop c1[n-1];
163            drop c2[n-1];
164            drop c3[n-1];
165            drop c4[n-1];
166            drop c5[n-1];
167            drop c6[n-1];
168            drop c7[n-1];
169            drop c8[n-1];
170            drop c10[n-1];
171            drop c11[n-1];
172            drop c12[n-1];
173            drop c13[n-1];
174            drop c14[n-1];
175            drop c15[n-1];
176
177
178
179
180     reset data Qprev,time;
181
182     let time:=n;
183
184
185     #let wQ:=0.001;
186
187     # Set new previous values
```

```
188
189     let Qprev[1] := Q[1];
190     let Qprev[2] := Q[2];
191     let Qprev[3] := Q[3];
192     let Qprev[4] := Q[4];
193     let Qprev[5] := Q[5];
194     let Qprev[6] := Q[6];
195     let Qprev[7] := Q[7];
196     let Qprev[8] := Q[8];
197     let Qprev[9] := Q[9];
198     let Qprev[10] := Q[10];
199     let Qprev[11] := Q[11];
200     let Qprev[12] := Q[12];
201     let Qprev[13] := Q[13];
202     let Qprev[14] := Q[14];
203     let Qprev[15] := Q[15];
204     let Qprev[16] := Q[16];
205
206
207
208     option solver bonmin; # Choose BONMIN as the solver (assuming that
209                           # bonmin is in your PATH
210
211
212     options bonmin_options "bonmin.allowable_gap 0.0009999
213     bonmin.time_limit 300 bonmin.nlp_log_level 0 bonmin.num_resolve_at_root 10
214      max_iter=100" ;
215
216      #bonmin.cutoff 5000000
217
218     option log_file ("logg_cont_new/run"&run&"/asklog"&run&time&".log");
219
220
221          option presolve 0;
222
223
224     solve;                # Solve the model
225
226     print cost > ("logg_cont_new/run"&run&"/cost"&run&time&".log");
227     print{j in 1..16} V[j] > ("logg_cont_new/run"
228                         &run&"/voltage"&run&time&".log");
```

```
229     print{j in 1..16} delta[j] > ("logg_cont_new/run"
230                          &run&"/delta"&run&time&".log");
231     print{j in 1..16} P[j,time] > ("logg_cont_new/run"
232                             &run&"/power"&run&time&".log");
233     print{j in 1..16} Q[j] > ("logg_cont_new/run"
234                       &run&"/reactive"&run&time&".log");
235     print{j in 1..16} Qprev[j] > ("logg_cont_new/run"
236                           &run&"/prev"&run&time&".log");
237     print{j in 1..16} Qswitch[j] > ("logg_cont_new/run"
238                         &run&"/switch"&run&time&".log");
239     print{j in 1..16} Qsvc[j] > ("logg_cont_new/run"
240                         &run&"/svc"&run&time&".log");
241     print _total_solve_elapsed_time > ("logg_cont_new/run"
242                             &run&"/time"&run&time&".log");
243
244     display case;
245     display time;
246     }
```

Bibliography

[1] Pierre Bonami and Jon Lee. Bonmin users' manual. 2009.

[2] Pierre Bonami, Jon Lee, Lorenz T. Biegler, Conn Andrew R., Gerard Cornujols, Ignacio E. Grossmann, Carl D. Laird, Andrea Lodi, Nicolas Sawaya, Francois Margot, and Andreas Wachter. Ibm research report - an algorithm framework for convex mixed integer nonlinear programs. 2005.

[3] Milan S. Calovic. Modeling and analysis of under-load tap-changing transformer control systems. *IEEE Transactions on Power Apparatus and Systems*, PAS-103(7):1909–1915, July 1984.

[4] Milan S. Calovic. Transmission alternatives for offshore electrical power. *Renewable and Sustainable Energy Reviews*, (13):1027–1038, 2009.

[5] COIN-OR. Computational infrastructure for operations research. `http://www.coin-or.org/`, 2011.

[6] David Crossley. Smart metering, load control and energy-using behaviour. 2007.

[7] Claudia DAmbrosio. Application-oriented mixed integer non-linear programming, 2009.

[8] Hassan Fletcher. The path of the smart grid. *IEEE Power & Energy Magazine*, 2010.

[9] Roger Fletcher and Sven Leyffer. Solving mixed integer nonlinear programs by outer approximation. *Mathematical Programming*, 66:327–349, 1994.

[10] John Forrest and Robin Lougee-Heimer. Cbc users guide. `http://www.coin-or.org/Cbc/cbcuserguide.html`, 2005.

[11] Robert Fourer, David M. Gay, and Brian W. Kernighan. *AMPL: A Modeling Language For Mathematical Programming.*

[12] John J. Grainger and William D. Stevenson, Jr. *Power System Analysis.* McGraw-Hill, 1994.

[13] Fuji Electric Group. Fuji electric review - thermal power plants. *FEe-Front runners*, 51(3), 2005.

[14] Erik Lundegaard Hannisdal. Statnett - automatic voltage control, power system modeling, 2010.

[15] Arne T. Holen, Olav B. Fosso, and Karstein J. Olsen. Tet4115 power system analysis tet5100 power engineering updates.

[16] D. P Kothari and I. J. Nagrath. *Power System Engineering.*

[17] H. Lefebvre, D. Fragnier, J.Y. Boussion, P. Mallet, and M. Bulot. Advantages of coordinated secondary voltage control in a deregulated environment.

[18] Sven Leyffer. Ac power flow and mixed-integer nonlinear optimization. June 2010.

[19] Jan Machowski, Janusz Bialek, and Dr. Jim Bumby. *Power System Dynamics: Stability and Control.*

[20] J. M. Maciejowski. *Predictive control with constraints.*

[21] Alexandra Von. Meier, Charles E. Leiserson, Ronald L. Rivset, and Clifford Stein. *Electric Power Systems - A Conceptual Introduction.* Wiley, 2001.

[22] James W. Nilsson and Susan A. Riedel. *Electric Circuits*.

[23] Jorge Nocedal and Stephen J. Wright. *Numerical Optimization*.

[24] Nordel. Nordel. http://www.nordel.org/, 2011.

[25] NVE. Energistatus.

[26] Olje og energidepartmenentet. Fremskynder utrulling av ams i midt-norge. http://www.regjeringen.no/nb/dep/oed/pressesenter/pressemeldinger/2011/fremskyndet-utrulling-av-automatisk-stro.html?id=636048, 2011.

[27] Tor Onshus. Instrumenteringssystemer.

[28] Alexandre Oudalov. Coordinated control of multiple facts devices in an electric power system, 2003.

[29] J.P. Paul, C. Corroyer, P. Jeannel, J.M. Tesseron, Maury F., and A. Torra. Improvments in the organization of secondary voltage control in france. August 1990.

[30] Pike Reseach. Smart grid investment to total $ 200 billion worldwide by 2015. http://www.pikeresearch.com/newsroom/smart-grid-investment-to-total-200-billion-worldwide-by-2015, 2009.

[31] Terje Riis-Johnsen and Olofsson Maud. Om et felles svensk-norsk marked for elsertifikater. http://www.regjeringen.no/upload/OED/pdf\%20filer/Protokoll_fra_droftinger_h_2009_til_desember_2010.pdf, 2010.

[32] J.L. Sancha, J.L Fernandez, A. Corts, and J.T. Abarca. A multilevel voltage control system: Description, coodination procedures and simulation results. pages 1002–1008, August 1996.

[33] J.L. Sancha, J.L Fernandez, A. Corts, and J.T. Abarca. Secondary voltage control: Analysis, solutions and simulation results for the spanish transmission system. *IEEE Transactions on Power Systems*, 11(2):630–638, May 1996.

[34] Statnett SF. Fiks - funksjonskrav i kraftsystemet. `http://www.statnett.no/Documents/Nyheter_og_media/Nyhetsarkiv/2008/FIKS_\%20_GENERELL\%20DOK\%20-\%2012158\%E2\%80\%A6.pdf`, 2010.

[35] Statnett SF. Statnett sf. `http://www.statnett.no/`, 2010.

[36] Sigurd Skogestad and Ian Postlethwaite. *Multivariable Feedback Control*.

[37] Statnet. Nettutviklingsplan, 2010.

[38] Hongbin Sun, Qinglai Guo, Boming Zhang, Wenchuan Wu, and Jianzhong Tong. Development and application of system-wide automatic voltage control system in china.

[39] Bernard W. Taylor. *Introduction to Management Science*.

[40] Norges vassdrags-og energidirektorat. Import og eksport av kraft. `http://www.nve.no/no/kraftmarked/sluttbrukermarkedet/varedeklarasjon1/import-og-eksport-av-kraft/`, 2010.

[41] Vigerske. PhD thesis.

[42] Andreas Waechter. Introduction to ipopt. `http://www.coin-or.org/Ipopt/documentation/`, 2010.

[43] Laurence A. Wosley. *Integer Programming*. John Wiley & Sons, 1998.

[44] Gongxian Xu. Comparison of iterative iom approaches for optimization of biological systems under uncertainty. 2009.